THE RADIATION AND GEOGRAPHIC EXPANSION OF PRIMATES THROUGH DIVERSE CLIMATES

Jorge Avaria-Llautureo[1]✉, Thomas A. Püschel[2], Andrew Meade[1], Joanna Baker[1], Samuel L. Nicholson[3], Chris Venditti[1]✉

1. School of Biological Sciences, University of Reading, UK
2. Institute of Human Sciences, School of Anthropology & Museum Ethnography, University of Oxford, UK
3. Climate Geochemistry, Max Planck Institute for Chemistry, Mainz, Germany

✉ Corresponding authors: j.l.avaria@reading.ac.uk; c.d.venditti@reading.ac.uk

Abstract

One of the most influential hypotheses about primate evolution postulates that their origin, radiation, and major dispersals were associated with exceptionally warm conditions in tropical forests at northern latitudes (henceforth the *warm tropical forest hypothesis*). However, this notion has proven difficult to test given the overall uncertainty about both geographic locations and paleoclimates of ancestral species. By the resolution of both challenges, we reveal that early primates dispersed and radiated in higher latitudes, through diverse climates, including cold, arid, and temperate conditions. Contrary to expectations of the warm tropical forest hypothesis, warmer global temperatures had no effect on dispersal distances or the speciation rate. Rather, the amount of change in local temperature and precipitation substantially predicted geographic and species diversity. Our results suggest that non-tropical, changeable environments exerted strong selective pressures on primates with higher dispersal ability – promoting the primate radiation and their subsequent colonization of tropical climates millions of years after their origin.

Significance Statement

Textbooks often portray primates as originating, evolving, and dispersing exclusively within warm tropical forests. This tends to come from fossil evidence distributed across northern latitudes typically characterized as tropical. However, accumulating independent evidence suggests that non-tropical climates were common across these regions during early primate evolution. By employing a new, advanced geographic model capable of inferring ancestral locations within a phylogenetic framework, we find that, contrary to widespread assumptions, early primates primarily inhabited cold and temperate climates. This research suggests that primates evolved and dispersed through diverse climates before becoming largely confined to modern warm tropical forests.

Introduction

The idea that early primates – including both modern primates and those belonging the broader Euprimates clade (1) – originated, radiated, dispersed, and thrived in the tropical forests, has been the dominant narrative for more than four decades (2–18). It is often reported that the primate radiation dramatically expanded, both geographically and taxonomically, in association with the global warming of the Paleocene-Eocene Thermal Maximum (PETM), when the range of the tropical forest presumably reached high latitudes in the Holarctic continents (5–7, 14, 19–22). We henceforth refer to these collective notions as the *warm tropical forest hypothesis* – i.e. that warm tropical forests have been instrumental in defining the primate radiation. The fact that the current distribution of extant primate species is largely restricted to a narrow range of tropical temperatures is also used to bolster support for the warm tropical forest hypothesis. However, current paleoclimatic evidence derived both from spore-pollen fossils and general circulation model simulations does not indicate tropical climates at the key locations where early fossil primates have been discovered or in the continents where they most likely originated (23–25). For example, climate reconstructions indicate that the Bighorn Basin and Chalk Butte in North America, as well as key fossil-bearing sites in Western Europe, were not tropical, before and during the PETM (23).

The apparent discrepancy between the expectations of the warm tropical forest hypothesis and that early primate fossils are found in non-tropical climates could stem from two factors. First, there are inherent temporal, spatial, and taphonomic biases in the fossil record. These biases have made the warm tropical forest hypothesis a longstanding challenge to evaluate. This is because the fossil record may tell us about the places, times, and, most importantly, the climates where fossilisation was most likely – rather than where primates evolved and diversified. That is, a higher probability of fossilization in non-tropical climates (26) could lead to the apparent lack of tropical climates in the early fossil record of primates. Second, despite the prevalent notion of warm tropical forest origins of primates, there is still considerable ambiguity in the terminology used to define and classify climate. Indeed, previous work on primate paleo-environments (27) has noted the extent of this issue: "*it seems that every work on the paleoecology of ape's environments adopts one or other of the numerous classifications of vegetation structure, never the same"*. A non-exhaustive literature search retrieves at least 10 names associated with the type of climate where primates are proposed to have originated – all incorporating concepts like tropical, warm, and wet: tropical rainforest (5), tropical climate (6), tropical flora (4), continuous evergreen forest belt (7), tropical plants (14), lush forest (14), paratropical forest (5), tropical angiosperm biome (15), warm forest (16), and wet forest (16).

Here, we overcome the enduring difficulty of evaluating the warm tropical forest hypothesis through the resolution of two main problems. Firstly, we combine climatic inferences from the fossil record with inferences based on the location of common ancestors – i.e. internal nodes within the most recent and comprehensively sampled Euarchonta phylogeny (28). To do this, we use a novel version of the Geographic (Geo) model implemented in BayesTraits v4 (29, 30) that accounts for historical inhabitable environments (e.g. ancient seas) – as well as incorporating phylogenetic and topological uncertainty (see Methods). Such an approach complements data derived from fossils and extant species distributions as it can reveal hitherto unknown historical climates in unsampled regions where primates and their ancestors lived. Ancestral species could have dispersed over vast distances, potentially up to about 20,000 kilometres in just 20,000 years (7). And secondly, after extracting geographical data, it was essential to use a formal and standard climate classification criterion to make the hypothesis testable and reproducible, avoiding the ambiguity and complexity of climate definitions found in the literature. It is possible to achieve this by using climatic data derived from the Hadley centre general circulation Coupled Model (Methods) (31–33) to classify the paleoclimates using the Köppen-Geiger (KG) classification system (34, 35).

Our approach brings the unique opportunity to explicitly and quantitatively test the various predictions made by the longstanding warm tropical forest hypothesis. If ancestral species evolved and relied on tropical forests for their dispersal, we would expect to find most early phylogenetic nodes to be reconstructed within the KG climate category *Tropical* (the type "A" climate, Fig. S1A and b) (34). The Tropical climate category refers to an environment that is hot all year round with average annual temperature over 18 °C (34, 35). This climate includes multiple subcategories: *Tropical Rainforest* (wet), *Tropical Monsoon* (short dry season), and *Tropical Savannah* (distinct dry season), which each differ in the annual amount and pattern of rainfall (34, 35). Since the KG Tropical category encompasses a wide variety of sub-climate categories, we are adopting a conservative approach in what constitutes a tropical climate. Furthermore, if early primates dispersed greater distances during the warmest global conditions of the PETM – when the tropical forests reached their widest latitudinal extension (5, 19, 36) – we would expect to observe a negative association between the total distance travelled across the globe for each species (pathwise, from root to tip - henceforth $D_{PATHWISE}$) and time (Fig. S1C). Similarly, we expect to observe a positive effect of global mean temperature on $D_{PATHWISE}$ (Fig. S1E, F). If early primates were also more speciose during the PETM, we would expect to observe a negative association between pathwise node count (the number of nodes between the root of the phylogenetic tree and every fossil and extant species, henceforth $NC_{PATHWISE}$) and time (Fig. S1D). $NC_{PATHWISE}$ can be regarded as a speciation rate metric (37). Finally, we should observe a positive effect of global mean temperature on $NC_{PATHWISE}$ (Fig. S1G, H).

To test these predictions, we carried out phylogenetic generalized least squares (PGLS) models using $D_{PATHWISE}$ as the response variable, with time and global temperature as predictors. Then, we carried out phylogenetic generalized linear mixed models (38) (PGLMM) using the same predictors but using $NC_{PATHWISE}$ as response variable with a Poisson distribution (Methods).

Results

Crown primates' ancestral location and paleoclimate

Using a single median phylogenetic tree (from a set of 100 median dated trees reconstructed in this study; Fig. S2; Methods), the geographic distribution of the most recent common ancestor of crown primates was inferred to have existed within North America in 8 of 10 Geo analyses. In the other two models, Western Europe was the most likely location. When we ran the analyses on the full set of 100 median phylogenetic trees, incorporating both topological and branch length uncertainty, we found North America as the location for the common ancestor in 70% of trees, and Western Europe in the other 30% of trees (Supplementary Text, Table S1). Those two likely locations are expected if we consider the location of some of the earliest fossil primates such as *Teilhardina magnoliana* and *T. brandti* in North America (19, 39), and *T. belgica* in Western Europe (40).

However, there is controversy as to the continental origins of primates owing to their almost synchronous first appearances in the fossil records of Asia, Europe, and North America (7, 19). Some previous research has additionally suggested that primates could have originated in Africa (41). Thus, we explicitly compared the model fit of each of these four potential continental origins (Fig. 1A, B) by running four additional models, each assigning one of four paleo-continents to the node representing the primate common ancestor and global paleomaps for all the other nodes in the tree. We ran 10 Geo analyses for each of the four models. Comparison of these models based on marginal likelihoods estimated by stepping-stone sampling (42) (Methods), showed that the model where the common ancestor was restricted to fall within North America was statistically preferred (Bayes Factor > 5; strong evidence; Fig. 1B) – this agrees with previous findings (39, 43). Finally, when we ran the Geo model on 200 down-sampled input data sets (Data S1) in which we mitigate sampling biases by reducing the number of fossils included from higher latitudes (see Supplementary Text), we still obtained North America as the most likely location for the common ancestor in 80% of the 200 data sets (Data S2).

The monthly paleotemperature and paleoprecipitation extracted from the posterior distribution of coordinates for the common ancestor in North America, indicates a cold KG climate category, classified as "D" (Fig. 1A). The Cold climate category is defined by a wide range of temperatures through the year, with temperatures of the hottest month over 10°C and temperatures of the coldest month equal to or lower than 0°C. The cold climate can also include years with dry summers (Ds), dry winters (Dw), or no dry season (Df). Within cold climates without dry seasons, it is still possible to find hot summers (Dfa) in which the summer temperature is equal to or over 22°C, and warm summers (Dfb) in which the temperature is over 10°C and equal to or lower than 22 °C for more than 4 months a year (34, 35). The climate subcategory for the primate common ancestor was the "Dfa" type (See Supplementary Material).

Historical climatic transition

Our climate reconstructions across phylogenetic nodes reveal that the dominant climate inhabited by ancestral species changed dramatically through time (Fig. 2A, B). Such a changeable climate is contrary to the general notion that primates mostly relied on tropical climates (5). Rather, we show that most early primates occupied cold, temperate, and dry climates (Fig. 2A, B). This result does not support a major expectation of the warm tropical forest hypothesis, i.e., a climate reconstruction of all or most of the early phylogenetic internal nodes falling within a Tropical KG climate (Fig. 2A).

Our patterns of climatic reconstruction stand over the full set of 100 phylogenetic trees (Data S3), which means that our results are robust to topological and divergence-time uncertainty in the phylogenetic tree, and to the uncertainty of ancestral locations inferred with the Geo model (Table S1). Our ancestral climatic reconstruction remains qualitatively similar even when we ran all the analyses on the 200 down-sampled data sets that are heavily biased against non-tropical fossils in northern latitudes (Supplementary Text, Data S1 and Data S2). If the taphonomic bias favouring fossilization in non-tropical climates was influencing our node climates to be reconstructed as non-tropical, then we should observe an increase of tropical climates across phylogenetic nodes when running the analyses on input data that randomly down sample the non-tropical fossils; but this expectation was not supported by the evidence (Data S2). Contrary to this expectation, the results show that there was an enduring major representation of non-tropical climates across all nodes corresponding to early

primate history, across all the 200 data sets (Data S2). This means that, even when the input data sets for the Geo model analyses are heavily biassed towards tropical fossils, our inferred pattern of ancestral climates is maintained.

Notably, our down-sampled datasets included the random removal of several species with uncertain phylogenetic positions such as *Ekgmowechashalidae*, and we also obtained similar results when including or excluding all the fossils with problematic phylogenetic position like *Parvimico materdei*, *Dolichocebus annectens,* and *Ucayalipithecus perdita* (Data S4, Data S5). We can therefore conclude that these species of questionable origin are not influencing our results.

Then, looking at the change in climate along branches (i.e., between main KG climate categories; arid, cold, temperate, and tropical, Fig. 2A) we see that climate transitions are relatively rare. Specifically, only 22% of phylogenetic branches showed such a transition from ancestral to descendant node. However, sub-climatic (Data S6) transitions are relatively more common (39% of branches). Within the ~22% of branches that showed transitions between main KG climate categories, the most common ones were from arid to tropical (~5% of branches), followed by tropical to temperate (4% of branches) (Fig. 3A). The least frequent transitions were from tropical to cold, and from cold to tropical (< 1 % of branches; Fig. 3A). Transitions from cold to any other climates were also rarely observed (< 2 % of branches; Fig. 3A). Transitional branches were associated with longer geographic dispersal distances (median distance for transitional branches = 561 km; median distance for non-transitional branches = 137 km), which means that major historical colonisation of novel climates (as defined by the main KG climate categories) was linked to long distance dispersals. Taken together, our results demonstrate that primates have had the ability to disperse and colonise diverse climates, where longer dispersal distances have tended to be associated with major climatic transitions.

To delve further into the historical transition between main KG climate categories and to provide a comprehensive understanding of its temporal pattern, we elaborate on the transitions across three temporal windows, namely, from 66 to 47.8 Mya (early), 47.8 to 23.03 (middle), and 23.03 to the present (late; Fig. 3B, C, and D). Most of the transitions in the early primate radiation were from the cold to the temperate climate (Fig.3B). In the middle of the radiation, most of the transitions occurred from the temperate to the arid climate (Fig. 3C). During the late radiation, major transitions occurred from the arid to the tropical climate (Fig. 3D). This late radiation pattern occurred seemingly coeval to a global trend towards drier and cooler climates of the Neogene (since 23.03 Mya), and the expansion of the major mid-latitude deserts (e.g., Saharo-Arabia). During the Neogene, the Earth cooled and experienced the onset of ice sheet expansion and expansion of the Mid-Latitude deserts. Perhaps such climatic changes may have caused the dispersals and transitions into tropical climates (44–46).

Global temperature is decoupled from biogeographic movement and speciation

Time had a significant positive effect on both $D_{PATHWISE}$ and $NC_{PATHWISE}$ (Table S2), meaning that dispersal distances and speciation rates were higher towards the present. This result is expected by virtue of the fact that longer-lived primate lineages have had more time to move and speciate -this is why it is important to account for the effect of time when evaluating the effect of additional covariates (like *GT*) in the regressions.

When we evaluated the effect of *GT* on $D_{PATHWISE}$ and $NC_{PATHWISE}$ while accounting for time, we did not find a significant effect on either of the two response variables (Table S2). These results do not support the warm tropical forest hypothesis expectation, i.e., that the past warmer global temperatures, including those of the PETM, were associated with the highest species dispersal distances and speciation rates (Fig. S1E).

GT may not explain primate biogeographic movement and speciation because of the natural mismatch between global and local environmental conditions (Fig. S3). Thus, perhaps local environmental conditions like local temperature (*LT*) and local precipitation (*LP*) specific to the region where each species lives or lived might relate positively to $D_{PATHWISE}$ and $NC_{PATHWISE}$. To assess this expectation, we tested the effects of *LT* and *LP* in our phylogenetic regression models. Such local variables were obtained from paleocoordinates for fossils, and from current coordinates for extant species (Methods). Our results show that *LT* had a significant effect on both response variables (positive on $D_{PATHWISE}$, negative on $NC_{PATHWISE}$; Table S2), which is in line with our expectation. *LP*, on the other hand, had a significant negative effect on $NC_{PATHWISE}$ only (Table S2). However,

the effect size of *LT* and *LP* was less than 3% of the variance in $D_{PATHWISE}$ and $NC_{PATHWISE}$ (Table S3). The relatively low amount of variance explained means that there is still uncertainty about what the main factors are that have driven the dispersal and speciation of primates across multiple continents.

The rate of change in *LT* and *LP* substantially explains dispersal and speciation

It has been proposed that the rate of climate change could be a factor of paramount importance in determining the geographic and evolutionary dynamics of primates (20, 47–51). In fact, during the PETM, *GT* not only increased to one of highest on record but also those increases were exceptionally fast (46, 52). Also, our results show that ancestral species dispersed and transitioned across diverse KG climatic subcategories (Data S6), which differ substantially in the annual pattern of both *LT* and *LP* (34, 35). Examining the local climatic variables allows us to explicitly test if changeable local environments in a species' history influenced $D_{PATHWISE}$ and $NC_{PATHWISE}$. Therefore, we tested the effect of the rate of local climate change on species dispersal and speciation by including the pathwise rate of local temperature (LT_{RATE}) and the pathwise rate of local precipitation (LP_{RATE}) as additional factors in our phylogenetic regressions (Methods). LT_{RATE} and LP_{RATE} are the cumulative change of *LT* and *LP* across the phylogenetic branches linking the common ancestor of all primates with every fossil and extant species, divided by time (Methods; though the effect of these variables is identical when we do not divide by time). Crucially, these changes are not directional, i.e., changes can be to either cooler, warmer, drier, or wetter local conditions.

We found that the effect size of LT_{RATE} and LP_{RATE} was 19% and 2% for $D_{PATHWISE}$, respectively (Table S3). Both rates of local changes related positively to $D_{PATHWISE}$ (Fig. 4B and C), which means that primates dispersed longer distances when the *LT* and *LP* changed at higher rates, irrespective of changes to warmer or colder temperatures or to drier or wetter conditions. On the other hand, the LP_{RATE} had a significant positive effect on $NC_{PATHWISE}$ (Fig. 4F, Table S2), explaining 14% of the variance (Table S3). This positive association means that primates diverged into new species more frequently when the total amount of annual *LP* changed at higher rates. When the local environment became drier or wetter, rapidly over time, speciation rate was higher.

The positive effect of LT_{RATE} and LP_{RATE} on dispersal and speciation was robust to several sources of uncertainty (see Methods). These sources of uncertainty include: the inferred ancestral locations reconstructed at phylogenetic nodes (Table S1, Table S4 and Table S5), the multiple continents proposed for primate origins (Table S1), the spatial variation in *LT* and *LP* (Table S4 and Table S5), and the uncertainty associated with the topology and branch lengths of the phylogenetic tree (Table S4 and Table S5).

Discussion

Our results suggest that early primates moved through, evolved, speciated, and went extinct in, as well as mostly lived in the non-tropical climates of the northern continents. Primates dispersed away from cold and variable climates, towards warmer and more stable ones. It was only late in their evolutionary history that primates colonised and diversified in tropical climates (Fig. S4). Our results are in stark contradiction to the warm tropical forest hypothesis that has prevailed for decades as the most likely explanation for primate origin and evolution (2, 5). This discrepancy is mainly attributable to bringing a new generation of phylogenetic and biogeographical methodologies to bear on the question of primate biogeography and its links to climate. These methods have the potential to realistically infer past geographical movement across the continents. In turn, this means that we can reveal climates outside the range of those seen in extant species – something which is not possible with other methods. In addition, our ability to extract local rather than global environmental conditions can explain why our results do not show strong support for the warm tropical forest hypothesis. Fig. S3 shows how divergent the local temperature has been from the global temperature during the primate radiation. Taken together, our approach allows us to test the warm tropical forest hypothesis in a far more nuanced fashion than has ever before been possible.

The novel idea that most early primates inhabited cold climates across high latitudes may seem to be at odds with fossil evidence concerning the paleoclimates of northern latitudes around 55 Mya. For instance, fossil evidence from Canada's high Arctic suggests a mild temperate climate during the early to middle Eocene, with winter temperatures at or just above freezing, summer temperatures reaching ≥ 20 °C, and high precipitation (53). However, using the KG classification system, the fossil evidence agrees with our results. Our results show

that the common ancestor of primates inhabited cold climates with no dry seasons and hot summers (Dfa, Data S6); which is defined by summer temperatures equal or over 22 °C (34, 35). The take-home message here is that warm temperatures alone are not enough evidence to support a tropical or temperate climate, and that fossil and paleoclimate data can define similar climates when the data is classified under the same criterion.

In the context of the effect of temperature on primate dispersal and evolution, we observe a clear, direct effect of local temperature, whereas global temperature shows no meaningful effect owing to their divergent patterns during the primate radiation. Specifically, local temperature fell below the global mean early in the radiation and rose to above-average levels during the middle and later stages (Fig. S3). The differential effect of local versus global temperature on primate evolution may help understand why important primate adaptations are decoupled from global temperature. For example, the fossil record shows that primate body size evolution was unaffected by periods of global cooling, periods of global warming, and relatively stable periods (54). To test hypotheses linking body size evolution with temperature - like the Cope-Bergmann hypothesis (55) - we should place more emphasis on the direction and rate of local temperature changes (56).

Local geographical location and climate are critically important for making inferences about the physiological nature of the primate common ancestor. This information can provide previously unknown clues to help us understand how the common ancestor might have lived and thrived in its ecological context. It is possible that hibernation or torpor might have been a survival strategy to thrive in such cold and seasonal conditions (57). This idea finds support in several small primates that live in unpredictable environments with freezing winter temperatures. For example, dwarf lemurs (genus *Cheirogaleus*) exist in cold climates with scarce resources by entering continuous hibernation for several months (57). Specifically, the highland-dwelling dwarf lemurs *C. crosleyi* and *C. sibreei*, dig themselves into the ground for hibernation beneath a soft layer of plant roots, humus, and leaves, where they are protected from freezing temperatures (57, 58). Whether the earliest primates were able to enter either torpor or hibernation is still debated (57), but some studies suggest that they could, possibly owing to having exceptionally low metabolic rates given their inferred small size (12). Small primates have high energy needs per unit of body mass and typically depend on scarce resources that are rich in energy, such as insects, small vertebrates, saps, and gums (12, 14). Given this, the primates' common ancestor could have lived in environments with low overall productivity or marked seasonality by lowering their metabolic rate or by temporally abandoning their normal homeothermic state (12).

Our results have implications for some of the main hypotheses proposed to explain primate origins. For example, the visual predation (2) and terminal branch feeding (4) hypotheses postulate that the adaptations that set modern primates apart from other mammals evolved as a response to dietary specialization. Both assume that selective processes took place in a warm, wet, and tropical forest environment. However, our results, supporting a cold climate, suggest that this dietary specialization - whether for visual predation or for plant products – might have occurred in forests adapted to cold rather than tropical climates. Some studies suggest that the origin of mammalian clades might be linked to the radiation of rosids (59), an angiosperm clade that includes many orders well-adapted to temperate climates and cold temperatures outside the tropics (60). Indeed, fossils of rosid plants, which are characteristic of coniferous and mixed forest ecosystems, have been found in North America around 66 million years ago (61), in the region we found most likely to be the primate common ancestor origin. Future work might seek to find a direct link between the geographical movement of these angiosperm taxa and primates. Such a connection would lend more support to the notion that primate origins were influenced by mixed forest environments

This study presents a novel view of primates biogeographic and evolutionary history. We highlight the idea that the prevalence of extant primates highly adapted to warm and stable tropical climates are the result of a long evolutionary process that started with selection on ancestral species thriving in a variety of colder and more seasonal paleoclimates of the northern latitudes (Figs. 1 and 2). From this colder and more seasonal local paleoenvironmental setting, the surviving species that started to diversify were those species able to disperse longer geographic distances, toward different - but more stable climates (Fig. 2).

The potential main selective force on dispersal ability was the rate of local environmental changes in temperature and precipitation, which we find to have both substantially predicted longer dispersal distance (Table S3). This result agrees with inferences made from individual-based models that explore the effect of rates of climate change on dispersal evolution (62). By assuming that species track geographically shifting conditions, these models show that under rapid rates of local climate change, species evolve to have higher dispersal capacity (62). Given that populations can cross large landscape gaps, this evolutionary process in turn could increase the rate of speciation by range fragmentation. To explain the remainder of the variance in primate dispersal capacity and speciation rates, it may be of interest to look at the extent to which other ecological and geographic factors, like body mass and geographic range size, relate to dispersal and speciation over long evolutionary timescales (63–65).

Finally, we can logically hypothesize that the evolutionary failure of early primates (and Plesiadapiformes; Fig. S5, Table S6), living in the colder and more fluctuating climates of the northern continents, was caused by their inability to keep moving towards warmer and more stable climates when their local environment changed too fast. As the main changes in driving species dispersal and speciation were not directional, then early species did not become extinct from global cooling (i.e., directional change to lower global temperatures) or forest contraction and disintegration in northern latitudes (i.e., directional changes to habitat reduction)(16). Consequently, species with a higher capacity to disperse from places with challenging and volatile environments are the only ones that have left their evolutionary trace in contemporary primate diversity.

Methods

Phylogenetic trees

Our comparative analyses were based on the most complete phylogeny of Euarchonta to date (28). This phylogeny includes 902 tips of which 419 are extant and 483 are fossils (Data S5). The Primates clade (excluding the incertae sedis *Altanius orlovi* (14)) contains 404 extant and 361 fossil tips. To address issues associated with zero-branch lengths and both temporal and topological uncertainty, we dated a random sample of 100 of the total set of most parsimonious topologies (MPTs) obtained by Wisniewski et al. (28), using a slightly modified version of their tip-dating procedure (28) and implemented in BEAST2 (66).

For each of the 100 MPTs, we obtained a posterior sample of dated trees from which we retrieved a single representative by calculating a median tree using the Kendall-Colijn metric (67) (Data S7). After removing potentially problematic taxa (see Supplementary Text), this set of 100 median trees contains 894 tips spanning Euarchonta (Data S8). We conducted the comparative analyses based on each on these 100 median trees, and on an additional median tree calculated from the 100 median trees. We also conducted all comparative analyses after additionally excluding *Parvimico materdei*, *Dolichocebus annectens,* and *Ucayalipithecus perdita* (Data S4) as they (probably erroneously) were recovered as stem anthropoids (28). Finally, we conducted all comparative analyses on the original median tree available in Wisniewski et al. (28) (Data S5) for comparison. Results across all phylogenies were qualitatively similar (Data S5).

Geographic distribution data

We obtained geographic coordinates (longitude and latitude) for every phylogenetic tip in order to infer the posterior distribution of coordinates at ancestral phylogenetic nodes.

For extant species, we downloaded distribution polygons from the IUCN Red List of Threatened Species (68) and generated a random sample of coordinates within each polygon. This approach allowed us to get an exhaustive representation of the extent of the geographic distribution for each species. There were three species in the tree which were absent from the IUCN database: *Lepilemur mittermeieri, Microcebus mittermeieri,* and *Otolemur crassicaudatus.* For each of these, we obtained their polygons using the Map of Life database (69). We defined the number of random of coordinates to generate based on the polygons geographic area (Table S8). This data set for all coordinates is available as Data S9.

For most fossil species, we downloaded paleogeographic coordinates from the PBDB (61). For fossil species with no information in the PBDB, we obtained present-day coordinates from the localities where the fossils were found. Then, we reconstructed their paleogeographic coordinates using the “reconstruct” function of the

chromosphere R package, version 0.4.1 (70), the PALEOMAP model (71), and both their first appearance date (FAD) and last appearance date (LAD). We randomly adjusted co-ordinates for sister taxa which fell within <50m of one another (see Supplementary Text). The complete coordinate data set for fossils is available as Data S10.

Ancestral locations inference

We inferred the posterior distribution of coordinates at ancestral phylogenetic nodes using a novel approach of the Geo model (29) in BayesTraits version 4 (30). The previous version of the Geo model reconstructed the posterior distribution of nodal longitude and latitude using a three-dimensional Cartesian coordinates system (x, y, and z) that considers the spherical nature of Earth. It estimates the posterior distribution of ancestral coordinates while sampling across all the coordinates within the geographic range of species. This approach avoids the potential biases of using one coordinate per phylogenetic tip such as is often done using geographic centroids, mid latitudes, or longitudes. Changes in coordinates across the branches of the phylogenetic tree are modelled using Brownian motion which assumes that species disperse across the globe at a constant speed (distance over time). However, the Geo model can also estimate ancestral locations while considering continuous variation in dispersal speed across phylogenetic branches. The speed of movement ranges from species quiescence (no movement per unit time), through constant movement in direct proportion of the passage of time (Brownian motion), to heterogeneous long-distance dispersals per unit time. Estimations of the speed of species' dispersal across phylogenetic branches are based on the variable rate model (72). The variable rate model detects shifts away from a constant (background) speed expected under Brownian motion. We compared the constant and variable speed models by means of Bayes Factors (BF). The BF is calculated as double of the difference of the log marginal likelihoods of two models - estimated by stepping stone sampling in BayesTraits while considering the number of parameters of the model (i.e., model complexity) (42). Higher log marginal likelihoods represent better fitted models and by convention, $BF > 2$ indicates positive support, $BF = 5–10$ indicates strong support, and $BF > 10$ is considered very strong support for a model over the other (73).

In this study, we introduce a novel extension to the original Geo model (29) that restricts reconstructed locations to points found only on land (33) Initially, all reconstructed locations are placed on land, and when proposing a new location, the closest point to the proposed location is identified on the map. If the closest point is found to be in the sea, the new location is assigned as zero probability (rejected), otherwise it is accepted or rejected based on its likelihood. Geography is not static through time; therefore, maps were created for different time periods (see below). As the phylogeny is time calibrated each internal node is assigned a map based on its age.

To restrict the space for ancestral location inferences, we used maps from the PALEOMAP project (71), which contains global maps for every million years, during the last 1,100 million years. We matched every phylogenetic node with the closet paleomap given their ages. With this approach we ensured that the reconstructed longitudes and latitudes for the phylogenetic internal nodes fell within the ancestral configuration of continents. The ability to restrict reconstructions to valid paleocordinates means that, for the first time, we could consider continental drift in the reconstruction of the primates' ancestral geographic locations. Simulations demonstrate that the new model version accurately recovers ancestral locations (Supplementary Text and Fig. S6).

We ran 10 MCMC chains of 800 million iterations each, discarding the first 600 million iterations as burn in. We also ran four analyses where we restricted the paleomap for the node representing the crown Primates. We selected the four continents proposed as the ancestral location for the crown Primates: Asia, Africa, Europe, North America. We ran 10 MCMC chains of 800 million iterations for each of the four model restrictions, discarding the first 600 million iterations as burn in. Then we compared all models by using Bayes Factors. Usually, when Europe is suggested as the place of origin for the common ancestor of primates, it is implicitly included within the coarser continental area of Eurasia (28, 74). This coarse discretization of Earth is a common practice given the limitations of biogeographical models that use discrete tip data in the phylogenetic tree. However, we leverage the higher geographical resolution of the Geo model to evaluate whether either Europe or Asia is a possible location for the origin of crown primates.

Global paleotemperature

We extracted the global average temperature for every million years from Scotese et al. (52) to evaluate its expected positive effect on the primate radiation and geographic dispersal.

12-month paleoprecipitation and paleotemperature

We obtained global values of monthly precipitation and mean monthly surface temperature for a period spanning the entire evolutionary history of Euarchonta given the dates of both the median and set of phylogenetic trees, i.e., up to around 76 million years ago. We used three approaches to get the monthly precipitation and temperature for extant, fossil, and phylogenetic nodes, respectively.

For extant species, we extracted monthly precipitation and temperature values from their geographic centroids from the WordClim Version 2 (75). We estimated the species geographic centroid within their IUCN and MOL polygons, using the terra R package, version 1.7.71 (Data S11).

For fossil species, we obtained the monthly paleoprecipitation and paleotemperature values from their paleocoordinates (Data S10) using world paleoclimatic simulations based on the Hadley centre general circulation Coupled Model (HadCM3). Here we use the HadCM3BL-M2.1aD model: see Supplementary Text for a full description of this scheme. We used the FAD and LAD of each fossil to consider match paleoclimatic layers to the fossils (Supplementary Text).

Finally, for the internal phylogenetic nodes, we extracted the monthly paleoprecipitation and paleotemperature (matched by age, as above) from the HadCM3BL-M2.1aD model. We used the posterior distribution of coordinates that were reconstructed with the Geo model. As there are many phylogenetic nodes in the median tree that do not match exactly the age of each climatic layer (given their difference in age resolution), we also extracted the paleoclimate data using the node ages from the sample of 100 phylogenetic trees. With this approach we considered the uncertainty in node ages when matching them with their closet simulated paleoclimate layers. All our results were qualitatively similar when running the analyses on the median tree and across the sample of 100 phylogenetic trees (see Robustness of results section below).

Köppen-Geiger climate classification

Using the monthly values of precipitation and mean monthly temperature for nodes, fossils, and extant species, we formally classified climates based on the Köppen-Geiger climate classification system (KG). The KG system classifies climates based on threshold values and seasonality of monthly air temperature and precipitation (34). It reflects climatic factors limiting vegetation growth and it aims to empirically map biome distributions around the world (34). The KG system classifies climates into five main categories. These main categories are: *Tropical* (A), *Arid* (B), *Temperate* (C), *Cold* (D), and *Polar* (E) climates – which are themselves divided amongst 30 subcategories (34, 35). For example, within the main category *Tropical*, there exists *Tropical Rainforest*, *Tropical Savannah*, and the *Tropical Monsoon* subcategories. The system can break down general terms that are equated in the hypothesis, such as "tropical" and "warm". Warm temperatures can define KG climates that are fundamentally different. For example, the climate classified as "Af" (*Tropical rainforest*) having temperatures over 18 °C all year round, is starkly different from the climate "Dfa" (*Cold, without dry season, and hot summer*) which has temperatures in the hottest month over 22 °C (34).

It is important to note that the climate concept used in this study differs from the environment concept. Climates are first-order processes for environments (i.e., processes that explain environment assuming a completely flat, non-variable landscape), but environments are also influenced by second-order processes such as focussed recharge, orography, topology, lithology etc. KG climates, for example, do not identify hydric wetlands and other microhabitat variability. Our approach allows us to separate the macro-scale first-order climatic processes influencing radiation and dispersal, but do not show fine details of environmental variability.

Finally, the KG classification has been widely applied to paleoclimate simulations (23, 24, 76). The KG system has several advantages over other climate classification systems in terms of applicability, comparability, and quantifiability (77). Figure S7 shows the world KG reconstructions for the present and for the past, using the WorldClim Version data, and the HadCM3BL-M2.1aD simulated paleoclimate data, respectively.

Here, we assigned KG climates following the revised KG climate classification of Peel et al (35) and using Wong Hearing et al.'s (76) R script.

Geographic distances moved from root to tip ($D_{PATHWISE}$)

We obtained a measure for the geographic distance that each primate species moved across the globe from the location of the most recent common ancestor (MRCA) of crown Primates (Data S12). For this, we added up the root-to-tip branchwise dispersal distance along phylogenetic paths, i.e., across all phylogenetic branches that link the MRCA with each tip in the median tree. First, we calculated the geographic distance per phylogenetic branch, using the Great Circle distance. For this measure, we used the median of the coordinates inferred with the Geo model (phylogenetic nodes), the median of inferred paleocoordinates (fossils) or the within-polygon centroids (extant species). Second, we added up the branch-wise distances along the paths linking the MRCA to the tip for each fossil and extant species.

Node count from root to tip ($NC_{PATHWISE}$)

To study speciation, we used node count (NC) along phylogenetic paths (Data S12). There are alternative non-model-based tip-rate metrics used to study speciation rate, such as the inverse of equal splits (ES) or the inverse of terminal branch length (TB) (37). However, we preferred to use NC as it has been shown to be less influenced by potential biases and sources of uncertainty associated with branch-length estimation from empirical data (78). NC captures the average speciation rate over the entire phylogenetic path and weights all branch lengths equally. We did not use speciation metrics estimated from time-varying birth–death diversification models owing to the erroneous inference of the general diversification patterns when the variation in rate of sequence evolution is not properly considered during the time-tree inference (79). Additionally, it has also been shown in the context of phylogenetic regressions that NC is the response variable that exhibits the highest statistical power when compared to regressions using ES or TB as speciation metrics (37).

Local precipitation and temperature rates of change (LP_{RATE} and LT_{RATE})

To get the total amount of change in temperature and precipitation along phylogenetic paths we used a three-step approach. First, we extracted the total local precipitation per year (LP) and the year-mean local temperature (LT). These data were extracted for the posterior coordinates of each phylogenetic node, and from the paleocoordinates for fossils and the geographic centroid for extant species (Fig. S8). Second, we calculated the absolute difference of the median LP and LT, between the ancestral and descendant node for each phylogenetic branch. Third, we summed the per branch absolute differences between LP and LT along the paths that link the common ancestor for each fossil and extant species. We divided this variable by the total time along each path (i.e. path length) given the median time-calibrated phylogenetic tree.

Phylogenetic regressions

We performed two sets of phylogenetic regression analyses to study the correlates of $D_{PATHWISE}$ and $NC_{PATHWISE}$. To study the correlates of $D_{PATHWISE}$, we used Bayesian phylogenetic generalized least squares regression models (PGLS), estimating Pagel's lambda in BayesTraits v4.

We first evaluated the effect of time and global average temperature (GT) on $D_{PATHWISE}$. Time was obtained from the path length of the time-calibrated median phylogenetic tree (Data S12). GT is available across the Phanerozoic at a resolution of one million years and was obtained from Scotese et al. (52). We extracted the GT from all the paleocoordinates (given their FAD and LAD) for fossil tips, and from the centroid within the polygon for extant species (Data S12). We matched the fossils and extant coordinates with the GT values, according to their age.

Then, we evaluated the effect of local precipitation (LP) and local temperature (LT) on $D_{PATHWISE}$. The LP and LT variables correspond to the annual precipitation and annual mean temperature values extracted from all the paleocoordinates for fossil tips (given their FAD and LAD), and from the centroid within the polygon for extant species (Data S12). The annual precipitation and annual mean temperature for fossil tips were extracted from the HadCM3BL-M2.1aD simulation layers. The annual precipitation and annual mean temperature for extant species was extracted from the WorldClim version 2 data. Finally, we evaluated the effect of LP_{RATE} and LT_{RATE} on $D_{PATHWISE}$.

To study the correlates of $NC_{PATHWISE}$ we performed phylogenetic generalized linear mixed models (PGLMMs) using the MCMCglmm R package 2.35 (38). We used a Poisson distribution to model $NC_{PATHWISE}$. As in the PGLS analyses $D_{PATHWISE}$, we tested the effect of time, GT, LP, LT, LP_{RATE}, and LT_{RATE}.

For the PGLS regression we ran 1,100,000 iterations, sampling every 1,000 iterations and discarding the first 100,000 iterations as burn in. Statistical significance of predictor variables was estimated based on a P_{MCMC} metric. This metric is based on counting the percentage of regression parameters that are higher (or lower) than zero in the posterior distribution. When the regression parameter is higher (or lower) than zero over 95% of the posterior distribution, then the predictor variable is statistically significant. For PGLMM regressions we also ran 1,100,000 iterations, sampling every 1,000 iterations and discarding the first 100,000 iterations as burn in. Regression coefficients were judged to be significant according to the P_{MCMC} metric estimated by the "MCMCglmm" R function.

Acknowledgments

We are grateful to Carolynne Roberts, Olivia Price, Kerry Stewart, Suzy White, George Butler, and Jacob Gardner, for helpful discussion. We would like to thank Veri Lobos Haoa for her work with the figures in this article. This work was funded by a Leverhulme Trust Research Leadership Award to CV (RL-2019-012).

References

1. M. T. Silcox, S. López-Torres, Major Questions in the Study of Primate Origins. *The Annual Review of Earth and Planetary Sciences is online at earth.annualreviews.org* **45**, 113–150 (2017).
2. M. Cartmill, Rethinking Primate Origins. *Science (1979)* **184**, 436–443 (1974).
3. M. Cartmilll, New Views on Primate Origins. *Evol Anthropol* 105–111 (1992).
4. R. W. Sussman, "Primate Origins and the Evolution of Angiosperms" (1991).
5. N. G. Jablonski, Primate homeland: Forests and the evolution of primates during the Tertiary and Quaternary in Asia in *Anthropological Science*, (2005), pp. 117–122.
6. J. G. Fleagle, C. C. Gilbert, "The Biogeography of Primate Evolution: The Role of Plate Tectonics, Climate and Chance" in *Primate Biogeography Progress and Prospects*, S. M. Lehman, J. G. Fleagle, Eds. (2006), pp. 375–418.
7. T. Smith, K. D. Rose, P. D. Gingerich, J. A. Sabloff, Rapid Asia-Europe-North America geographic dispersal of earliest Eocene primate Teilhardina during the Paleocene-Eocene Thermal Maximum. *Proc Natl Acad Sci U S A* **130**, 11223–11227 (2006).
8. Christophe. Soligo, O. A. Will, Simon. Tavaré, C. R. Marshall, R. D. Martin, "New Light on the Dates of Primate Origins and Divergence" in *Primate Origins - Adaptations and Evolution*, M. J. Ravosa, Ed. (Springer, 2006), pp. 29–49.
9. C. F. Ross, M. I. Hall, C. P. Heesy, "Were Basal Primates Nocturnal? Evidence from Eye and Orbit Shape" in *Primate Origins - Adaptations and Evolution*, M. J. Ravosa, Ed. (Springer, 2006), pp. 233–256.
10. M. Cartmill, P. Lemelin, D. Schmitt, "Primate Gaits and Primate Origins" in *Primate Origins - Adaptations and Evolution*, M. J. Ravosa, Ed. (Springer, 2006), pp. 403–435.
11. B. T. Shea, "Start Small and Live Slow: Encephalization, Body Size, and Life History Strategies in Primate Origins and Evolution" in *Primate Origins - Adaptations and Evolution*, Ravosa, Matthew J., (Springer, 2006), pp. 583–623.
12. J. J. Snodgrass, W. R. Leonard, M. L. Robertson, "Primate Bioenergetics: An Evolutionary Perspective" in *Primate Origins - Adaptations and Evolution*, M. J. Ravosa, Ed. (Springer, 2006), pp. 703–737.
13. C. Stringer, P. Andrews, *The complete world of human evolution*, Second (Thames & Hudson Ltd., 2011).
14. J. G. Fleagle, *Primate Adaptation & Evolution*, J. G. Fleagle, Ed., Third Edition (Academic Press, 2013).
15. C. Soligo, J. B. Smaers, Contextualising primate origins - an ecomorphological framework. *J Anat* **228**, 608–629 (2016).

16. B. Williams, Effects of Climate Change on Primate Evolution in the Cenozoic. *Nature Education Knowledge* **7** (2016).
17. D. Youlatos, D. Moussa, N. E. Karantanis, L. Rychlik, Locomotion, postures, substrate use, and foot grasping in the marsupial feathertail glider Acrobates pygmaeus (Diprotodontia: Acrobatidae): Insights into early euprimate evolution. *J Hum Evol* **123**, 148–159 (2018).
18. R. D. Martin, *Primate origins and evolution. A phylogenetic reconstruction* (Princeton University Press, 1990).
19. K. C. Beard, "The oldest North American primate and mammalian biogeography during the Paleocene-Eocene Thermal Maximum" (2008).
20. P. D. Gingerich, Environment and evolution through the Paleocene-Eocene thermal maximum. *Trends Ecol Evol* [Preprint] (2006).
21. S. Cachel, *Fossil Primates*, S. Cachel, Ed., First Edition (Cambridge University Press, 2015).
22. C. Soligo, Invading Europe: Did climate or geography trigger early eocene primate dispersals? in *Folia Primatologica*, (2007), pp. 297–313.
23. V. A. Korasidis, S. L. Wing, C. A. Shields, J. T. Kiehl, Global Changes in Terrestrial Vegetation and Continental Climate During the Paleocene-Eocene Thermal Maximum. *Paleoceanogr Paleoclimatol* **37** (2022).
24. A. Pohl, T. Wong Hearing, A. Franc, P. Sepulchre, C. R. Scotese, Dataset of Phanerozoic continental climate and Köppen–Geiger climate classes. *Data Brief* **43** (2022).
25. L. Burgener, E. Hyland, B. J. Reich, C. Scotese, Cretaceous climates: Mapping paleo-Köppen climatic zones using a Bayesian statistical analysis of lithologic, paleontologic, and geochemical proxies. *Palaeogeogr Palaeoclimatol Palaeoecol* **613** (2023).
26. A. Rosas, *et al.*, The scarcity of fossils in the African rainforest. Archaeo-paleontological surveys and actualistic taphonomy in Equatorial Guinea. *Hist Biol* **34**, 1582–1590 (2022).
27. P. Andrews, "Structure and composition of ape environments" in *An Ape's View of Human Evolution*, P. Andrews, Ed. (Cambridge University Press, 2015), pp. 69–81.
28. A. L. Wisniewski, G. T. Lloyd, G. J. Slater, Extant species fail to estimate ancestral geographical ranges at older nodes in primate phylogeny. *Proceedings of the Royal Society B: Biological Sciences* **289** (2022).
29. C. O'Donovan, A. Meade, C. Venditti, Dinosaurs reveal the geographical signature of an evolutionary radiation. *Nat Ecol Evol* **2**, 452–458 (2018).
30. M. Pagel, A. Meade, D. Barker, Bayesian estimation of ancestral character states on phylogenies. *Syst Biol* **53**, 673–684 (2004).
31. V. D. Pope, M. L. Gallani, P. R. Rowntree, R. A. Stratton, The impact of new physical parametrizations in the Hadley Centre climate model: HadAM3. *Clim Dyn* **16**, 123–146 (2000).
32. C. Gordon, *et al.*, The simulation of SST, sea ice extents and ocean heat transports in a version of the Hadley Centre coupled model without ¯ux adjustments. *Clim Dyn* **16**, 16–147 (2000).
33. P. J. Valdes, *et al.*, The BRIDGE HadCM3 family of climate models: HadCM3@Bristol v1.0. *Geosci Model Dev* **10**, 3715–3743 (2017).
34. H. E. Beck, *et al.*, Present and future köppen-geiger climate classification maps at 1-km resolution. *Sci Data* **5** (2018).
35. M. C. Peel, B. L. Finlayson, T. A. Mcmahon, "Updated world map of the Köppen-Geiger climate classification Hydrology and Earth System Sciences Updated world map of the Köppen-Geiger climate classification" (2007).
36. T. Smith, K. D. Rose, P. D. Gingerich, "Rapid Asia-Europe-North America geographic dispersal of earliest Eocene primate Teilhardina during the Paleocene-Eocene Thermal Maximum" (2006).
37. M. G. Harvey, D. L. Rabosky, Continuous traits and speciation rates: Alternatives to state-dependent diversification models. *Methods Ecol Evol* **9**, 984–993 (2018).
38. J. D. Hadfield, "MCMC Methods for Multi-Response Generalized Linear Mixed Models: The MCMCglmm R Package" (2010).
39. P. E. Morse, *et al.*, New fossils, systematics, and biogeography of the oldest known crown primate Teilhardina from the earliest Eocene of Asia, Europe, and North America. *J Hum Evol* **128**, 103–131 (2019).
40. D. L. Gebo, R. Smith, M. Dagosto, T. Smith, Additional postcranial elements of Teilhardina Belgica: The oldest European primate. *Am J Phys Anthropol* **156**, 388–406 (2015).

41. M. T. Silcox, “The Biogeographic Origins of Primates and Euprimates: East, West, North, or South of Eden?” in *Mammalian Evolutionary Morphology: A Tribute to Frederick S. Szalay.*, M. Dagosto, E. Sargis, Eds. (Springer-Verlag, 2008), pp. 199–231.
42. W. Xie, P. O. Lewis, Y. Fan, L. Kuo, M. H. Chen, Improving marginal likelihood estimation for bayesian phylogenetic model selection. *Syst Biol* **60**, 150–160 (2011).
43. J. I. Bloch, M. T. Silcox, D. M. Boyer, E. J. Sargis, “New Paleocene skeletons and the relationship of plesiadapiforms to crown-clade primates” (2007).
44. J. Zhang, *et al.*, Modeling the effects of global cooling and the Tethyan Seaway closure on North African and South Asian climates during the Middle Miocene Climate Transition. *Palaeogeogr Palaeoclimatol Palaeoecol* **619** (2023).
45. Z. Zhang, *et al.*, Aridification of the Sahara desert caused by Tethys Sea shrinkage during the Late Miocene. *Nature* **513**, 401–404 (2014).
46. J. Zachos, H. Pagani, L. Sloan, E. Thomas, K. Billups, Trends, rhythms, and aberrations in global climate 65 Ma to present. *Science (1979)* **292**, 686–693 (2001).
47. L. Zhang, *et al.*, Global assessment of primate vulnerability to extreme climatic events. *Nat Clim Chang* **9**, 554–561 (2019).
48. L. Sales, B. R. Ribeiro, C. A. Chapman, R. Loyola, Multiple dimensions of climate change on the distribution of Amazon primates. *Perspect Ecol Conserv* **18**, 83–90 (2020).
49. M. P. Pinto, R. Beltrão-Mendes, M. Talebi, A. A. de Lima, Primates facing climate crisis in a tropical forest hotspot will lose climatic suitable geographical range. *Sci Rep* **13** (2023).
50. X. G. Qi, *et al.*, Adaptations to a cold climate promoted social evolution in Asian colobine primates. *Science (1979)* **380** (2023).
51. J. M. Kamilar, L. Beaudrot, Effects of Environmental Stress on Primate Populations. (2018). https://doi.org/10.1146/annurev-anthro-102317.
52. C. R. Scotese, H. Song, B. J. W. Mills, D. G. van der Meer, Phanerozoic paleotemperatures: The earth’s changing climate during the last 540 million years. *Earth Sci Rev* **215** (2021).
53. J. J. Eberle, D. R. Greenwood, Life at the top of the greenhouse Eocene world- A review of the Eocene flora and vertebrate fauna from Canada’s High Arctic. *Bulletin of the Geological Society of America* [Preprint] (2012).
54. C. Soligo, Correlates of body mass evolution in primates. *Am J Phys Anthropol* **130**, 283–293 (2006).
55. G. Hunt, K. Roy, Climate change, body size evolution, and Cope’s Rule in deep-sea ostracodes. *Proceedings of the National Academy of Sciences* **103**, 1347–1352 (2006).
56. L. N. Wilson, *et al.*, Global latitudinal gradients and the evolution of body size in dinosaurs and mammals. *Nat Commun* **15** (2024).
57. M. B. Blanco, K. H. Dausmann, S. L. Faherty, A. D. Yoder, Tropical heterothermy is “cool”: The expression of daily torpor and hibernation in primates. *Evol Anthropol* [Preprint] (2018).
58. K. H. Dausmann, L. Warnecke, Primate torpor expression: Ghost of the climatic past. *Physiology* [Preprint] (2016).
59. H. Wang, *et al.*, Rosid radiation and the rapid rise of angiosperm-dominated forests. *Proceedings of the National Academy of Sciences* **106**, 3853–3858 (2009).
60. M. Sun, *et al.*, Recent accelerated diversification in rosids occurred outside the tropics. *Nat Commun* **11**, 3333 (2020).
61. M. D. Uhen, *et al.*, Paleobiology Database User Guide Version 1.0. *PaleoBios* **40** (2023).
62. J. Boeye, J. M. J. Travis, R. Stoks, D. Bonte, More rapid climate change promotes evolutionary rescue through selection for increased dispersal distance. *Evol Appl* **6**, 353–364 (2013).
63. A. Alzate, R. E. Onstein, Understanding the relationship between dispersal and range size. *Ecol Lett* **25**, 2303–2323 (2022).
64. J. Smyčka, A. Toszogyova, D. Storch, The relationship between geographic range size and rates of species diversification. *Nat Commun* **14**, 5559 (2023).
65. D. G. Jenkins, *et al.*, Does size matter for dispersal distance? *Global Ecology and Biogeography* **16**, 415–425 (2007).
66. R. Bouckaert, *et al.*, BEAST 2: A Software Platform for Bayesian Evolutionary Analysis. *PLoS Comput Biol* **10** (2014).
67. M. Kendall, C. Colijn, Mapping Phylogenetic Trees to Reveal Distinct Patterns of Evolution. *Mol Biol Evol* **33**, 2735–2743 (2016).

68. IUCN, The IUCN Red List of Threatened Species. Version 2022-2. https://www.iucnredlist.org. Accessed on [07/11/2022]. 2022 (2022).
69. W. Jetz, J. M. McPherson, R. P. Guralnick, Integrating biodiversity distribution knowledge: Toward a global map of life. *Trends Ecol Evol* **27**, 151–159 (2012).
70. Á. T. Kocsis, N. B. Raja, chronosphere: Earth system history variables. (2020). https://doi.org/10.5281/zenodo.3530703.
71. C. R. Scotese, N. Wright, PALEOMAP Paleodigital Elevation MOdels (PaleoDEMS) for the Phanerozoic PALEOMAP Project, EarthByte.
72. C. Venditti, A. Meade, M. Pagel, Multiple routes to mammalian diversity. *Nature* **479**, 393–396 (2011).
73. A. E. Raftery, "Hypothesis testing and model selection" in *Markov Chain Monte Carlo in Practice*, W. Gilks, S. Richardson, D. Spiegelhalter, Eds. (Chapman & Hall, 1996), pp. 163–187.
74. M. S. Springer, *et al.*, Macroevolutionary Dynamics and Historical Biogeography of Primate Diversification Inferred from a Species Supermatrix. *PLoS One* **7** (2012).
75. S. E. Fick, R. J. Hijmans, WorldClim 2: new 1-km spatial resolution climate surfaces for global land areas. *International Journal of Climatology* **37**, 4302–4315 (2017).
76. T. W. Wong Hearing, *et al.*, Quantitative comparison of geological data and model simulations constrains early Cambrian geography and climate. *Nat Commun* **12** (2021).
77. C. Yu, *et al.*, Climate paleogeography knowledge graph and deep time paleoclimate classifications. *Geoscience Frontiers* **14** (2023).
78. P. O. Title, D. L. Rabosky, Tip rates, phylogenies and diversification: What are we estimating, and how good are the estimates? *Methods Ecol Evol* **10**, 821–834 (2019).
79. A. Shafir, D. Azouri, E. E. Goldberg, I. Mayrose, Heterogeneity in the rate of molecular sequence evolution substantially impacts the accuracy of detecting shifts in diversification rates. *Evolution (N Y)* (2020). https://doi.org/https://doi.org/10.1111/evo.14036.

Figures

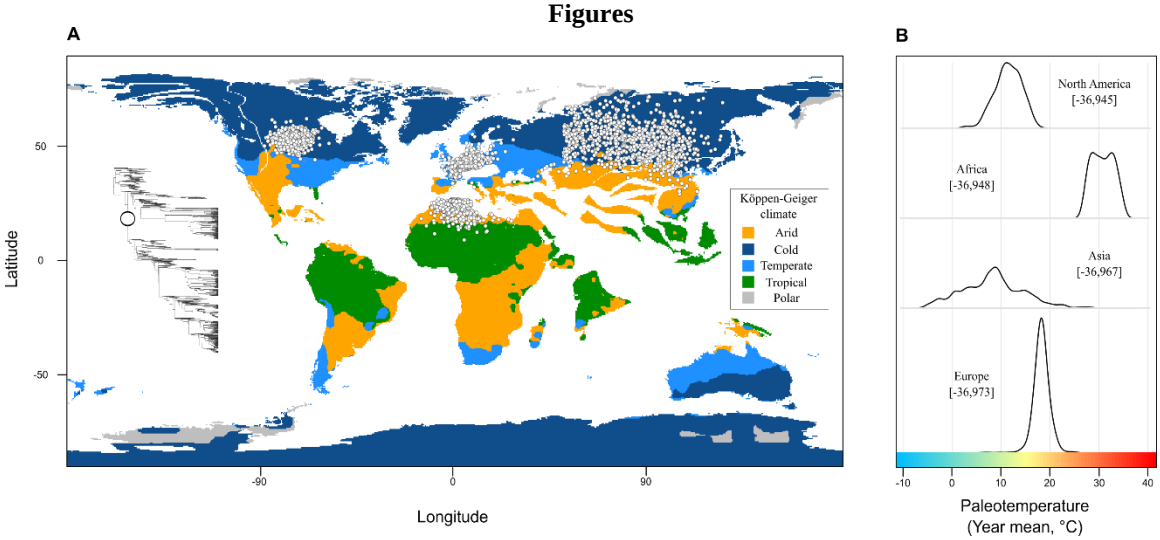

Figure 1. The common ancestor of Primates was found in a cold climate within North America. (A), world paleomap with the Köppen-Geiger main climates of 66 million years ago. White circles on the map are the posterior distribution of coordinates for the common ancestor (white circle on the tree). These coordinates were inferred using the Geo model with paleomap restrictions. We ran four Geo models, restricting the location to be either in North America, Africa, Asia, or Europe. (B), mean annual palaeotemperature extracted from the posterior distribution of coordinates across each continent. The continental locations are ordered by their marginal likelihood inferred by steppingstones (numbers in squared brackets), with the best fit model on top given the Bayes Factor model comparison.

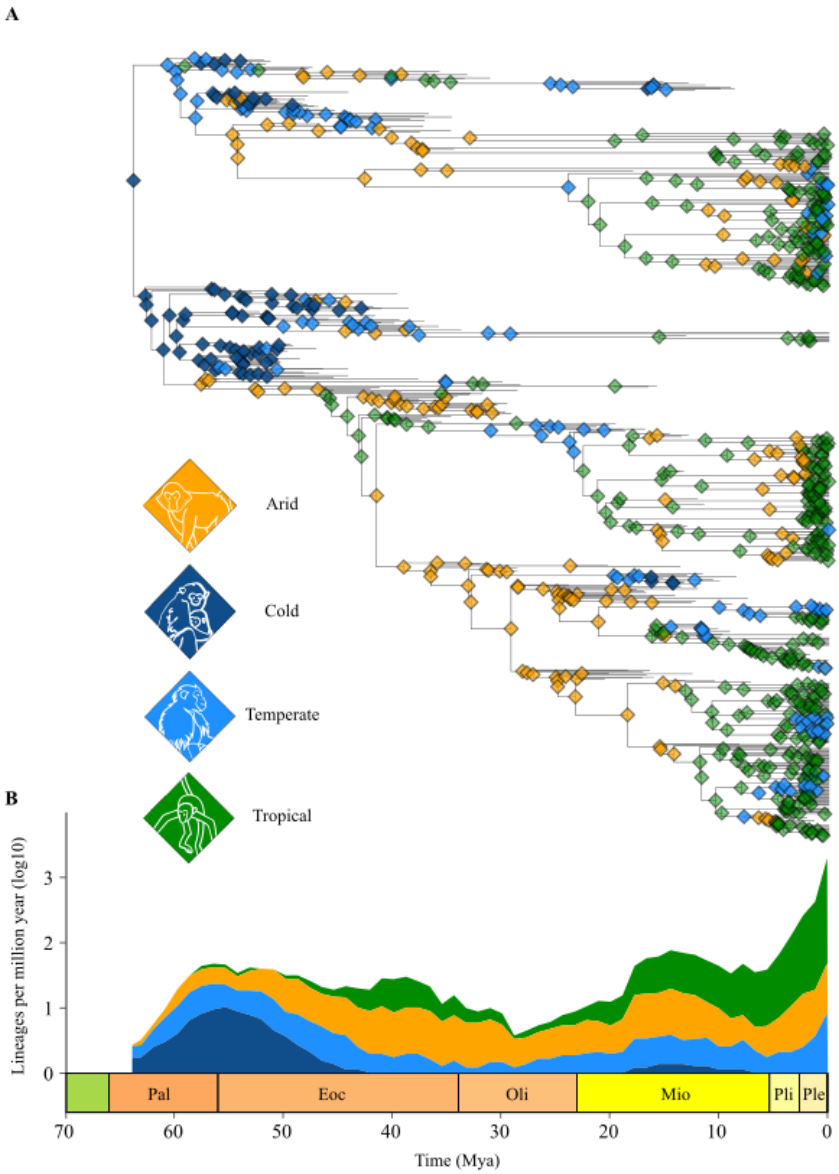

Figure 2. Primates evolved through diverse climates. (A), primate median phylogenetic tree with the Köppen-Geiger main climates categories for all internal nodes. The climate reconstruction was obtained by extracting the monthly palaeotemperature and paleoprecipitation (simulated under the HadCM3BL-M2.1aD climate model) from the Geo model posterior node coordinates. (B), lineages through time intervals of one million years. Fossils and extant species (phylogenetic tips) are also included in this plot. Colors represent the proportion of lineages inhabiting each climate category through time.

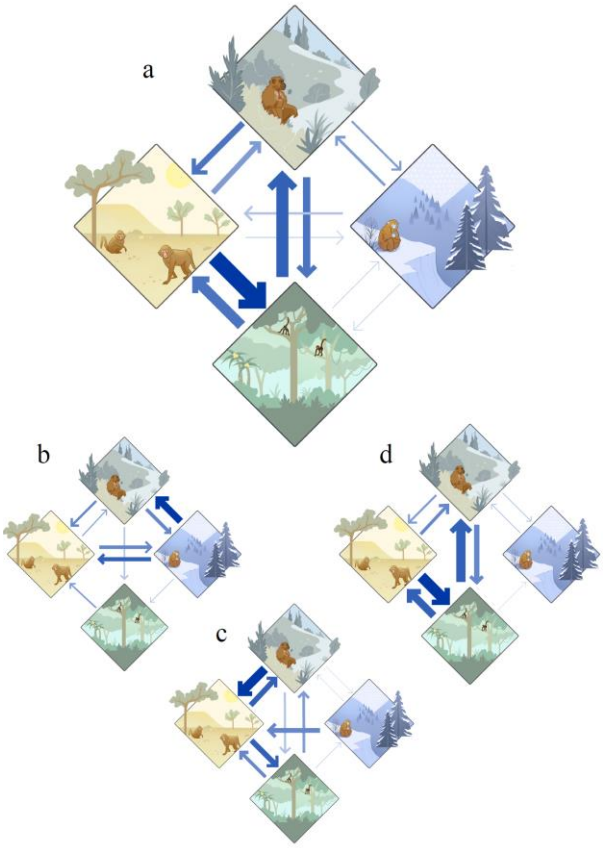

Figure 3. Primates historically transitioned across diverse climates. (A), transition between the Temperate (top), Arid (left), Tropical (bottom), and Cold (right), main climates, for all primates. Arrow size represents the proportion of phylogenetic branches with the respective transitions. (B), climatic transitions for early primates, who were living between 65 and 47.8 million years ago. (C), climatic transitions for species that were living between 47.8 and 23.03 million years ago. (D), climatic transitions for species that were living from 23.03 million years ago to the present.

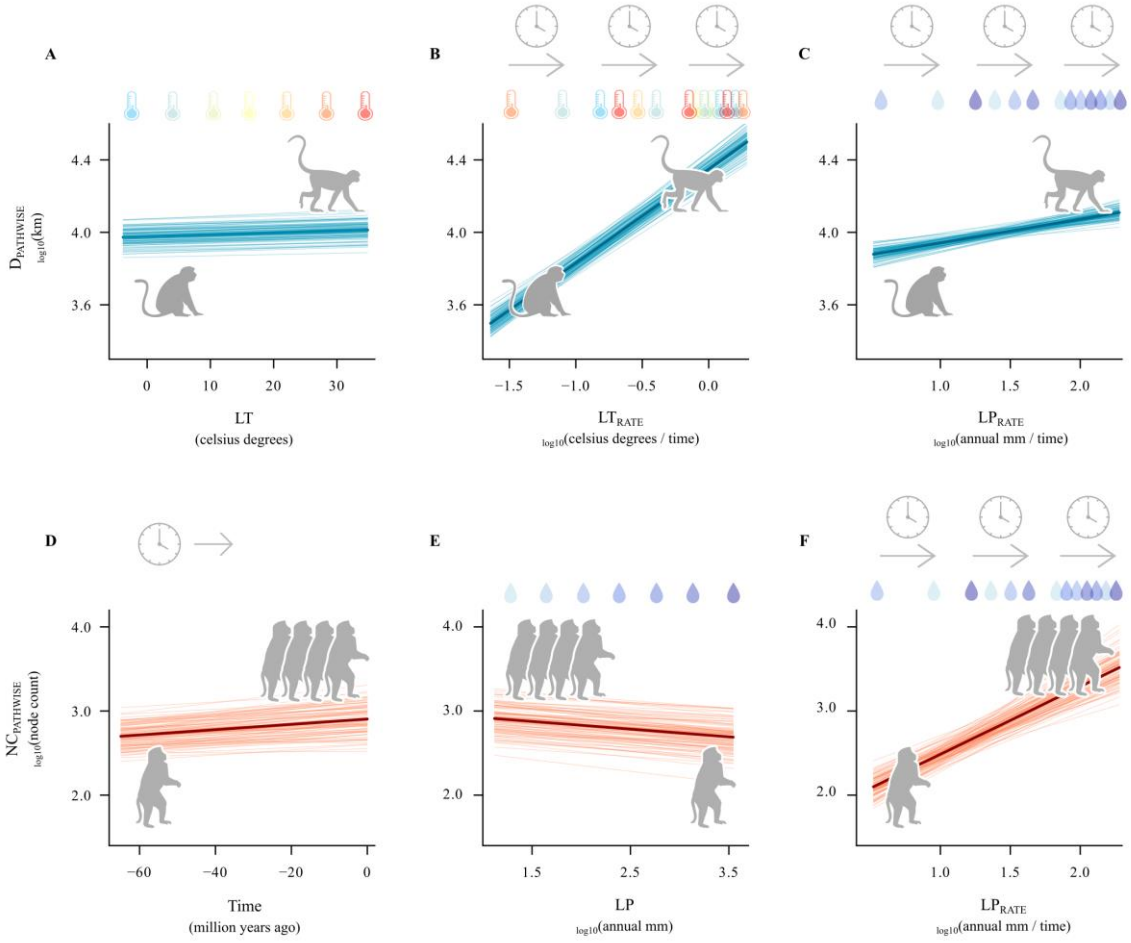

Figure 4. Primates dispersed and radiated under variable rates of change in local climate. (A), local temperature (LT) had a significant positive effect on pathwise distance ($D_{PATHWISE}$). (B), the pathwise rate of local temperature (LT_{RATE}) had a significant positive effect on $D_{PATHWISE}$. (C, F), the pathwise rate of local precipitation (LP_{RATE}) had a significant positive effect on both $D_{PATHWISE}$ and pathwise node count ($NC_{PATHWISE}$). (D), $NC_{PATHWISE}$ was positively associated with time. (E), local precipitation (LP) had a significant negative effect on $NC_{PATHWISE}$. We show the predictor variables that were significant in both the median and the sample of phylogenetic trees (see Methods). Light-colored lines represent the posterior distribution of phylogenetic regression slopes. Darker lines represent the mean slopes of the posterior distribution.

Supplementary Information

Dating a sample of Euarchontan phylogenies

Our analyses use the recently published Euarchonta phylogeny, originally built by Wisniewski et al. (1). The original analysis was a meta-analytical approach similar to the super tree method of matrix representation with parsimony (2). Their novel approach used a formal set of rules to accommodate phylogenetic uncertainty in source studies, removed redundant datasets or down-weighted datasets based on similar underlying matrices. They also reconciled taxonomic information to a common source (1, 3). However, the phylogeny of Wisniewski et al. (1) has several sources of uncertainty such that the authors highlight some caveats to using the tree for comparative analyses. Principally, the fossil *Catarrhini indet CPI-6487*, caused a "bizarre" reconstruction of South America as the continent of origin for the crown anthropoid ancestor (Catarrhini + Platyrrhini) (1). Additionally, the median phylogenetic tree of Wisniewski et al. (1) contains 117 branches with zero length (Data S5), which can be a source of bias in comparative analyses.

We dated the sample of 100 MPTs using a tip-dating procedure adapted from that used by Wisniewski et al. (1) and implemented in BEAST2 (4). We make just a few modifications to their procedure. Firstly, for each MPT, we restricted topology moves by setting the appropriate operators to have zero weight. Thus, we obtained a posterior distribution of trees with a single fixed topology but variation in divergence dates and branch lengths. We conditioned the fossilized birth-death process on the root, with a date calibration as described in Dos Reis et al. (5) ranging between 66 million years (the age of the oldest sampled fossil) and 130 million years (an absence of placental mammals). We additionally tested a model which calibrated on the origin of the birth-death process (using the same dates) but found no difference in the results. We set an exponential (mean =1) prior distribution for the sigma parameter of the log-normal rate distribution applied to estimate optimized relaxed clock rates, as recommended for groups with clock-like rates of molecular evolution and supported in the molecular data underlying this analysis (5). We restricted the mean clock rate to vary between 0.01 and 0.02, extending beyond the extremes of variation observed in Wisniewski et al. (1) to facilitate faster convergence (though our results are identical when this parameter was not restricted). For transition rates, we placed a gamma prior (α= 0.2, β = 0.5) and for transversion rates a gamma prior (α= 0.2, β = 0.25); this avoids the default priors which place a lot of weight on very small values. Finally, we placed a uniform prior ranging between 0 and 1 on the turnover rate and a beta distribution on the sampling proportion (α = 5, β=90). As BEAST2 does not work with multifurcations, all polytomies were randomly resolved before tip-dating; they were collapsed back to reflect the original input topology afterwards.

We removed three fossils (*Cercopithecini sp. Indet. AUH 1321*, *Colobinae indet. KNM-BN 1251*, and *Colobinae indet. KNM-TH 48368*) from our dating procedure. As these taxa had uncertain placement (see (1)), our preliminary analyses indicated that divergence dates were being heavily influenced (varying by tens of millions of years) by their inclusion (along with *Catarrhini indet CPI-6487*, see above). We also excluded four taxa from the analyses because their taxonomic relationships were particularly problematic or because we could not identify the specimen when these tips had the genus name only. These four tips are *Cantius UM 86543*, *Cheracebus purinus*, *Tupaia sp. UNSM 87244*, and *Dermoptera indet. Pkg 240* and *Pkg 335*. Finally, we edited 19 extant species names in the tree to match with the IUCN Red List of Threatened Species (6) nomenclature. We also edited seven extinct species names to match with the Paleobiology Database (PBDB) (7) nomenclature (Table S7).

Phylogenetic uncertainty

We evaluated the robustness of our results to several sources of uncertainty in our data. First, we evaluated the effect of divergence times and topological uncertainty (Table S1, Table S4, and Table S5) by running the Geo model analyses across the sample of 100 median phylogenetic trees (Data S8). Regarding the pattern of climatic reconstruction, we obtained qualitatively similar results across the 100 phylogenetic trees (Table S1, Table S4, Table S5, and Data S3). We also reconstructed the same climatic pattern on the sample of trees that excluded the potentially problematic tips *Parvimico materdei*, *Dolichocebus annectens*, and *Ucayalipithecus perdita* (Data S4) and on the original meta tree of Wisniewski et al. (30) (Data S5).

To evaluate the effect of phylogenetic uncertainty on our phylogenetic regressions results, we obtained all the response and predictor variables from each of the 100 trees in the sample. Those variables are the

$D_{PATHWISE}$, $NC_{PATHWISE}$, LP_{RATE}, and LT_{RATE}, Then, we ran the phylogenetic regression across each of the 100 median trees. We obtained qualitatively similar results. The variable LT, LT_{RATE}, and LP_{RATE} stand as the main drivers of primate dispersal distance (Table S4). The variables Time, LP, and LP_{RATE} stand as the main drivers for primate speciation rates (Table S5).

Adjustment of coordinates for closely associated fossils

Preliminary analyses using the Geographical (Geo) model with variable rates collapsed branches where sister tips had coordinates which were identical or within a Great Circle geographic distance (the shortest distance between two points on a sphere) of <50m. We therefore identified all instances where this scenario occurred in our tree and coordinate data. We found 10 fossils that matched the above-mentioned filtering criteria (duplicated coordinates or fell within <50m of their sister taxon). However, to keep these fossils in the median tree, we conducted an alternative approach that generated random coordinates for them. Namely, we created a circular polygon of 0.5 kilometres of radius from the central paleogeographic point where the fossil was found, and we generated 50 random coordinates within every circular polygon. The complete coordinate data set for fossils is available as Data S10.

Accuracy of ancestral location inferences with map restrictions

The new Geo model introduced in this study assigns zero-probability prior to coordinates located in the sea given the paleo- configuration of the continents, effectively ruling out the sea for node location inference. This prior is supported by the well-established evidence that primates are a land-adapted clade. To demonstrate the accuracy of this new extension of the Geo model, we simulated 1,000 node and tip coordinates using the phylogenetic section for extinct and extant species of New World monkeys. For each simulation, we randomly set the location for the root of the tree across the world's landmasses, and we assigned a mean variance of 18,000. We used this variance value as it was the similar to that estimated via our empirical analyses with the primate phylogeny and geographical data. Then, we ran the Geo model using the phylogenetic tree and the simulated tip coordinates as input data. Our results show that we recover the simulated data with high accuracy. This is demonstrated in Figure S6, as the simulated data (black points on the maps) fall within the posterior distribution of inferred coordinates (white points on the map).

General circulation model

For fossil species, we obtained the monthly paleoprecipitation and paleotemperature values from their paleocoordinates (Data S10) using world paleoclimatic simulations based on the Hadley centre general circulation Coupled Model (HadCM3). Specifically, we used the Bristol Lower Ocean resolution (BL), MOSES2.1a land surface exchange scheme (M2.1a), and fully dynamic vegetation model (D) (i.e., HadCM3BL-M2.1aD model) (8–11). The HadCM3BL-M2.1aD is a coupled General Circulation Model that considers the coupled circulation of the atmosphere and ocean, land surface exchange scheme, and vegetation dynamics. The performance of the HadCM3BL-M2.1aD in simulating modern climate is comparable to the current Coupled Model Intercomparison Project 5 and 6, state-of-the-art models (8, 9). The HadCM3BL-M2.1aD also recovers the pattern of global temperature change during the last 65 million years as expressed from fossil benthic foraminifera (12). General circulation models like the HadCM3BL-M2.1aD have been widely used in current paleoclimate research that have brought meaningful inferences about paleoclimate and diversity. Some examples include the FOAM and CESM models (13–17). We downloaded all the available monthly climatic layers in NetCDF format for 0 (the present), 4, 10, 14, 19, 25, 31, 35, 39, 44, 52, 55, 60, 66, 69, 75, and 80 million years ago. Then, we matched the fossil's paleocoordinates with the closet paleoclimate simulated layer, considering their ages. We then used the FAD and LAD of each fossil to consider the uncertainty of age-matching as the paleoclimatic layers have a lower age resolution than the fossils.

General circulation model uncertainty

Our KG climates reconstructed at phylogenetic nodes are dependent on temperature and precipitation data simulated with the HadCM3BL-M2.1aD model. Such simulations have associated errors, and they have a coarse temporal resolution (17 paleoclimate layers every 5 million years approximately). Therefore, we reconstructed ancestral climates by an alternative approach that excludes simulated layers - using a continuous time Markov model with variable transition rates (18) in BayesTraits v4. For this, we used the KG climates observed in all extant and fossil tips, categorized into four states: Tropical, Arid, Temperate,

and Cold. We estimated the ancestral climate using maximum likelihood on our median tree, and for each of the 100 trees in the sample. Then, we reconstructed the climate for each node by identifying the state with the highest likelihood. Finally, we compared these estimations with the estimation based on the HadCM3BL-M2.1aD at phylogenetic nodes. Results show qualitatively identical climates and transition patterns (Fig. S8).

Taphonomic bias

We evaluated whether the geographic overrepresentation of non-tropical fossils was biasing our inferences of ancestral climates by conducting sensitivity analyses. We ran the Geo model and classified the KG climates using several phylogenetic trees and data sets that were generated by sub-sampling non-tropical fossils (Data S1). We first classified the KG climates for all fossil paleocoordinates. As done previously, we used the fossil FADs and LADs to match them with the closest monthly climatic layer of the HadCM3BL-M2.1aD paleoclimate model. The fossil's climate classification given their FAD and LAD is available as Data 10.

Second, we selected one main KG climate for each fossil, for both their FAD and LAD. When having more than two main climates for one fossil, we selected the climate with highest representation across its geographic occurrences. When we had two main climates, we selected a climate at random. The final data sets are available as Data S1.

Third, we randomly sampled non-tropical fossils until we obtained the same proportion of the tropical fossils. For the KG fossil classification given their FADs, we obtained 73 tropical fossils and 285 non-tropical fossils (Data S1). Then, we obtained 10 random samples of non-tropical fossils with following sizes: 271, 249, 227, 205, 183, 161, 139, 117, 95, and 73 (same as tropical fossils). For the KG fossil classification given their LADs, we obtained 84 tropical fossils and 274 non-tropical fossils (Data S1). In total, we obtained 10 random samples of non-tropical fossils with following sizes: 264, 244, 224, 204, 184, 164, 144, 124, 104, and 84 (same as tropical fossils). This down-sampling procedure, given the FADs and LADs, was replicated 10 times, meaning that we analyzed 200 additional data sets in total (Data S1). With this approach we removed many tips with uncertain phylogenetic position like *Ekgmowechashalidae*.

If the fossil data was biasing the climate reconstruction of early primates, we should observe an increase in the number of tropical climates in early phylogenetic nodes as we decrease the representation of non-tropical fossils. Contrary to this expectation, the results show that there was an enduring major representation of non-tropical climates across all nodes corresponding to early primate history, across all the 200 data sets (Data S2). This means that, even when the input data sets for the Geo model analyses are heavily biassed towards tropical fossils, our inferred pattern of ancestral climates is maintained. Furthermore, the ancestral location for the crown Primates was inferred to be North America in 80% of those 200 data sets (Data S2).

Supporting References

1. A. L. Wisniewski, G. T. Lloyd, G. J. Slater, Extant species fail to estimate ancestral geographical ranges at older nodes in primate phylogeny. *Proceedings of the Royal Society B: Biological Sciences* 289 (2022).

2. M. A. Ragan, Phylogenetic inference based on matrix representation of trees. *Mol Phylogenet Evol* 1, 53–58 (1992).

3. G. T. Lloyd, G. J. Slater, A Total-Group Phylogenetic Metatree for Cetacea and the Importance of Fossil Data in Diversification Analyses. *Syst Biol* 70, 922–939 (2021).

4. R. Bouckaert, *et al.*, BEAST 2: A Software Platform for Bayesian Evolutionary Analysis. *PLoS Comput Biol* 10 (2014).

5. M. Dos Reis, *et al.*, Using phylogenomic data to explore the effects of relaxed clocks and calibration strategies on divergence time estimation: Primates as a test case. *Syst Biol* 67, 594–615 (2018).

6. IUCN, The IUCN Red List of Threatened Species. Version 2022-2. https://www.iucnredlist.org. Accessed on [07/11/2022]. 2022 (2022).

7. M. D. Uhen, *et al.*, Paleobiology Database User Guide Version 1.0. *PaleoBios* 40 (2023).

8. P. J. Valdes, *et al.*, The BRIDGE HadCM3 family of climate models: HadCM3@Bristol v1.0. *Geosci Model Dev* 10, 3715–3743 (2017).

9. P. J. Valdes, C. R. Scotese, D. J. Lunt, Deep ocean temperatures through time. *Climate of the Past* 17, 1483–1506 (2021).

10. V. D. Pope, M. L. Gallani, P. R. Rowntree, R. A. Stratton, The impact of new physical parametrizations in the Hadley Centre climate model: HadAM3. *Clim Dyn* 16, 123–146 (2000).

11. C. Gordon, *et al.*, The simulation of SST, sea ice extents and ocean heat transports in a version of the Hadley Centre coupled model without ¯ux adjustments. *Clim Dyn* 16, 16–147 (2000).

12. J. Zachos, H. Pagani, L. Sloan, E. Thomas, K. Billups, Trends, rhythms, and aberrations in global climate 65 Ma to present. *Science (1979)* 292, 686–693 (2001).

13. A. Pohl, T. Wong Hearing, A. Franc, P. Sepulchre, C. R. Scotese, Dataset of Phanerozoic continental climate and Köppen–Geiger climate classes. *Data Brief* 43 (2022).

14. V. A. Korasidis, S. L. Wing, C. A. Shields, J. T. Kiehl, Global Changes in Terrestrial Vegetation and Continental Climate During the Paleocene-Eocene Thermal Maximum. *Paleoceanogr Paleoclimatol* 37 (2022).

15. T. W. Wong Hearing, *et al.*, Quantitative comparison of geological data and model simulations constrains early Cambrian geography and climate. *Nat Commun* 12 (2021).

16. D. E. Ontiveros, *et al.*, Impact of global climate cooling on Ordovician marine biodiversity. *Nat Commun* 14 (2023).

17. L. N. Wilson, *et al.*, Global latitudinal gradients and the evolution of body size in dinosaurs and mammals. *Nat Commun* 15 (2024).

18. M. Pagel, Detecting correlated evolution on phylogenies: a general method for the comparative analysis of discrete characters. *Proc R Soc Lond B Biol Sci* 255, 37–45 (1994).

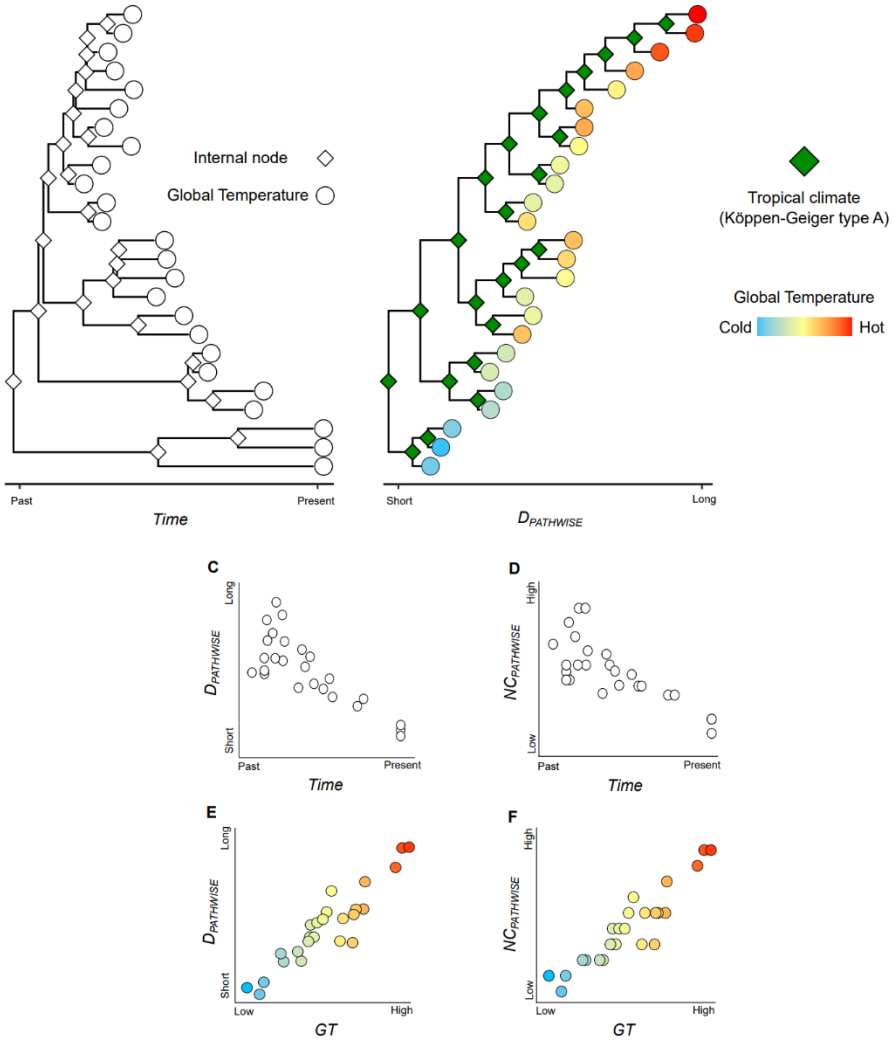

Fig. S1. Expected results in support of the warm tropical forest hypothesis. (A), time-calibrated phylogenetic tree of fossils and extant species. White-filled diamonds are the internal nodes (ancestral species). White-filled circles represent the global temperature that each species was experiencing at a respective time. (B), the time tree with branch lengths scaled according to the geographic distance each species dispersed. Green filled diamonds represent the Köppen-Geiger Tropical climate for ancestral species. Circles filled with color gradients represent the global temperature (*GT*). (C), the expected negative relationship between pathwise distance ($D_{PATHWISE}$) and time if early primates dispersed longer geographic distances. $D_{PATHWISE}$ is the sum of all the geographic distances across the branches that link the root of the tree with every phylogenetic tip. Time is the sum of all the branches that link the root of the time tree with every phylogenetic tip. (D), the expected negative relationship between pathwise node count ($NC_{PATHWISE}$) and time if early primates speciated at higher rates. $NC_{PATHWISE}$ is the number of nodes, or speciation events, between the root of the tree and every tip. (E), the expected positive relationship between $D_{PATHWISE}$ and *GT* if species dispersed longer distances during past warmer *GT*s. (F), the expected positive relationship between $NC_{PATHWISE}$ and *GT* if early primates speciated at higher rates during the past warmer *GT*s.

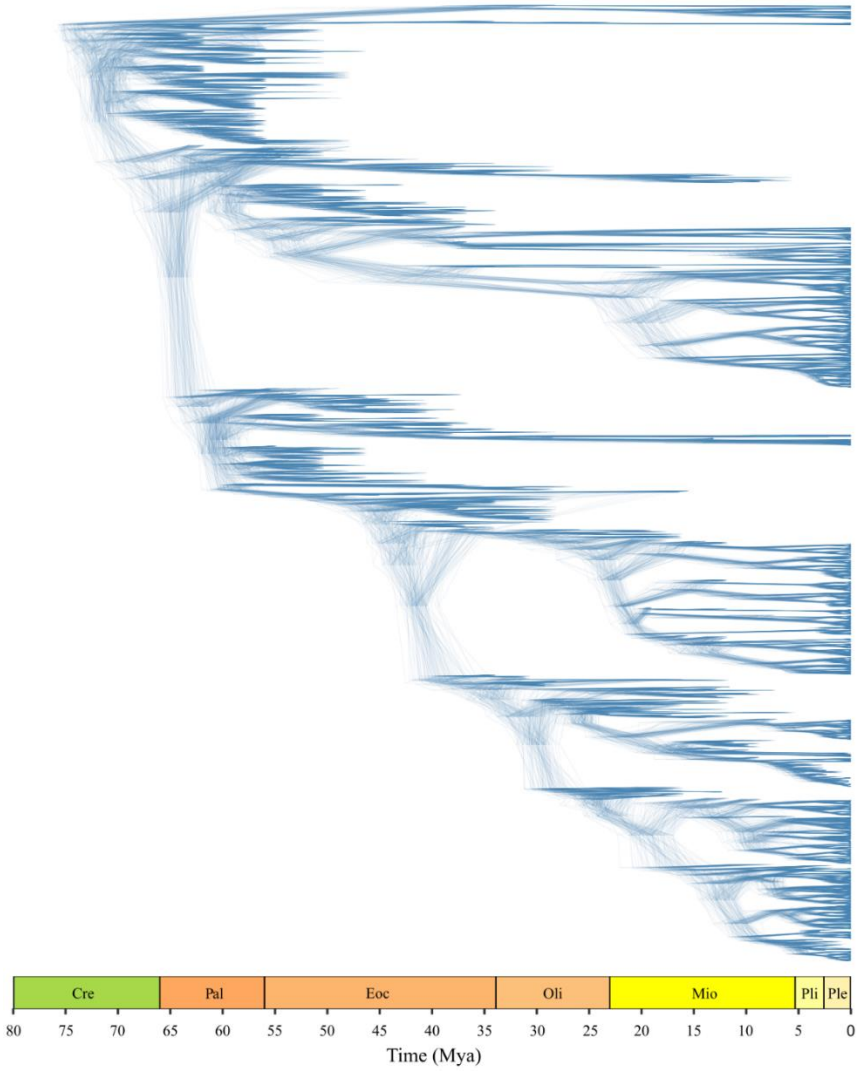

Fig. S2. DensiTree obtained from the sample of a 100 median dated MPTs. The median dated trees are stacked on top of each other and the structures of the trees are rotated to ensure the consistency of the tip order. The DensiTree includes the clade Euarchonta, (i.e., Primates, Pleasiadapiformes, Dermoptera, and Scandentia).

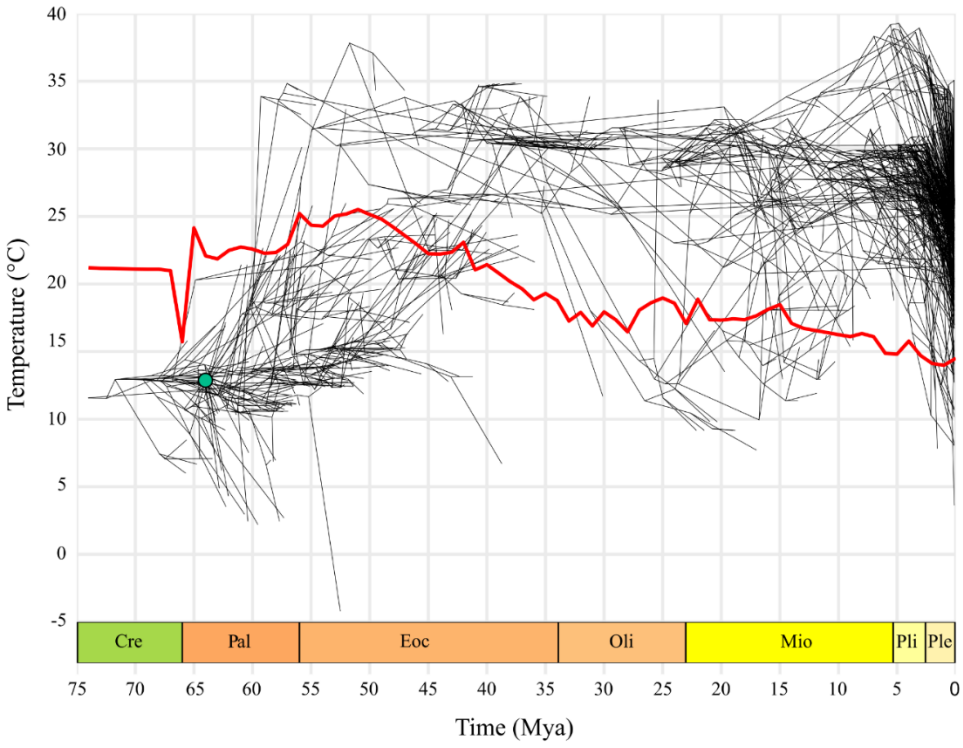

Fig. S3. Projected median phylogenetic tree of Primates and Plesiadapiformes in a space defined by annual mean local temperature (LT) and time. The LT at phylogenetic nodes corresponds to the median value across the locations extracted from the Geo model. LT at tips are the median values extracted from their observed occurrences. The red line indicates the global average temperature extracted from Scotese et al (2021). The green-filled point indicates the common ancestor of Primates.

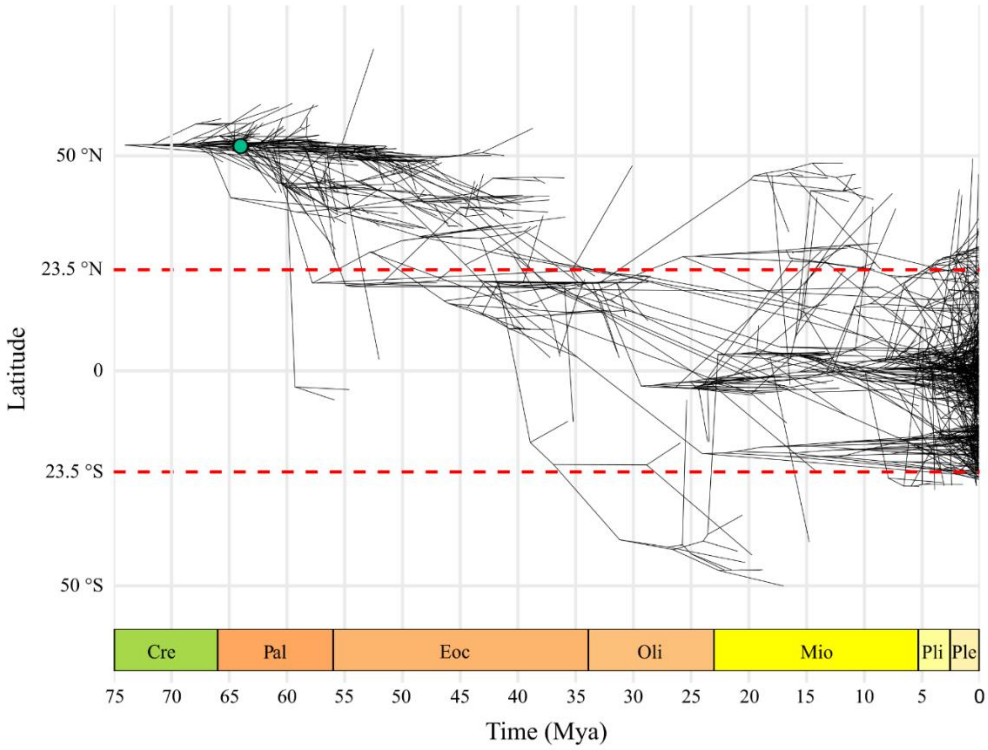

Fig. S4. Projected median phylogenetic tree of Primates and Plesiadapiformes in a space defined by latitude and time. The latitude at each phylogenetic node corresponds to the median value obtained from the Geo model analysis with paleo-map restrictions. Tip-latitudes are the median values obtained from observed occurrences. Red-segmented lines indicate the tropical region. Green-filled point indicates the common ancestor of Primates.

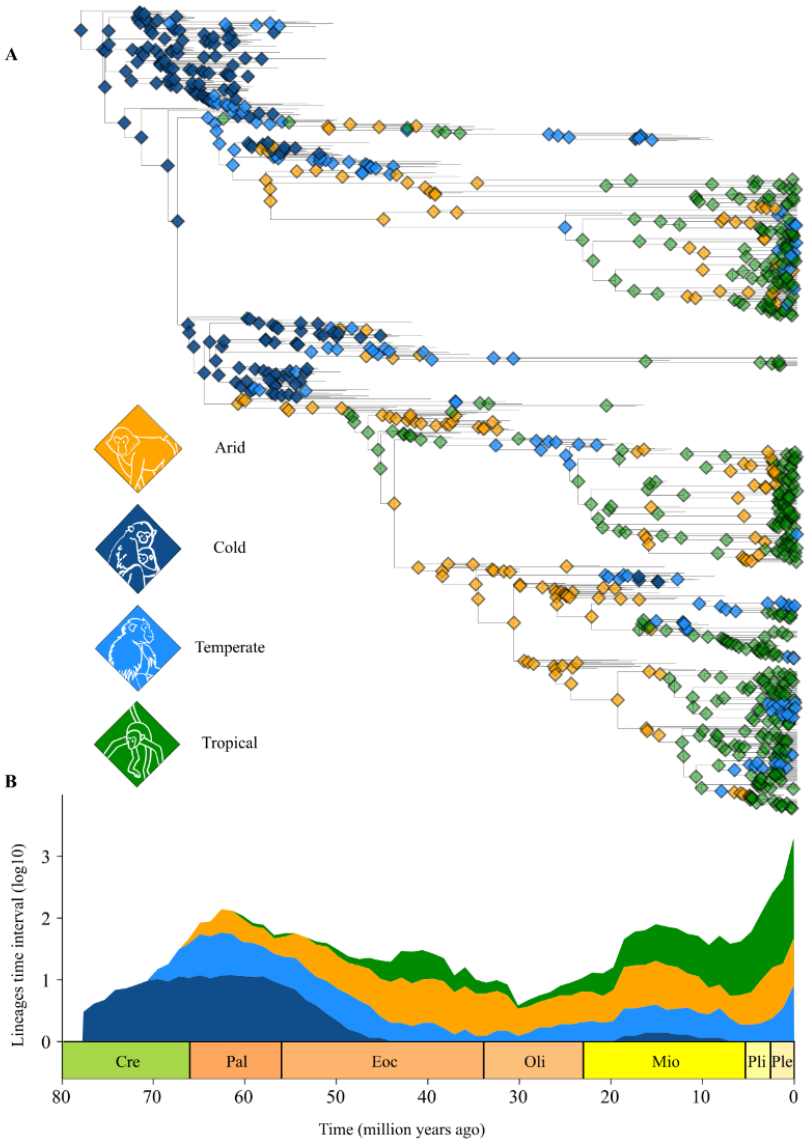

Fig. S5. Ancestral Plesiadapiformes and Primates inhabited diverse climates. (A), primates' median phylogenetic tree (including Plesiadapiformes) with the Köppen-Geiger main climate categories depicted for all nodes. The climate reconstruction was obtained by extracting the monthly palaeotemperature and precipitation (simulated under the HadCM3BL-M2.1aD climate model) from the Geo model posterior node coordinates. (B), lineages through time intervals of one million years. Fossil and extant species (phylogenetic tips) are also included in this plot. Colors represent the relative proportion of lineages inhabiting each climate category.

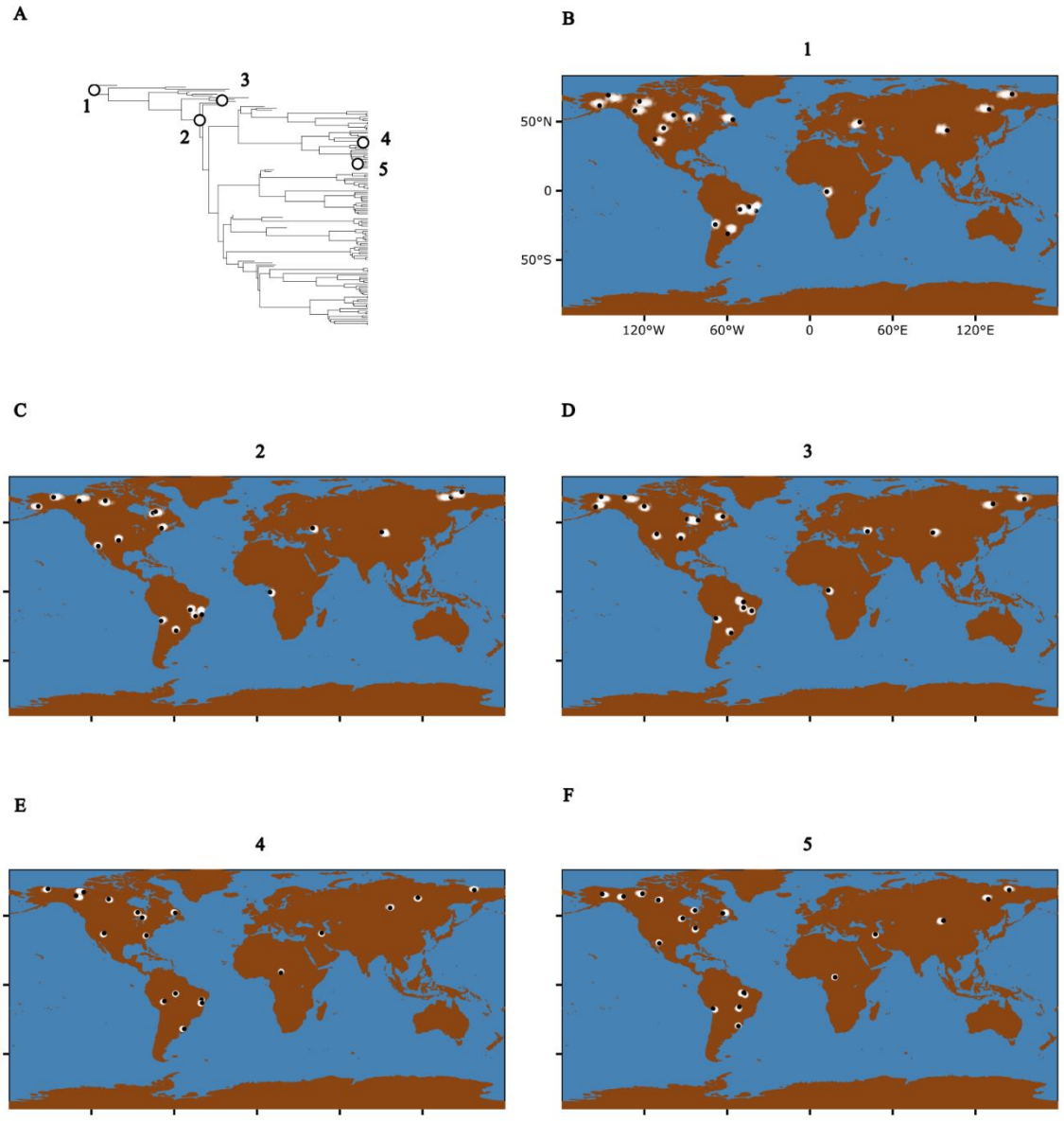

Fig. S6. Geo model with map restriction accuracy in ancestral location inference. (A), phylogenetic tree for New World monkey on which we ran 1,000 simulations for node and tip coordinates. (B-F), 20 random simulations for each of the five nodes selected at random. Black points on each map represent 20 random simulations for the respective node. White points on each map indicate the 20 random posterior distributions of ancestral locations for the respective node.

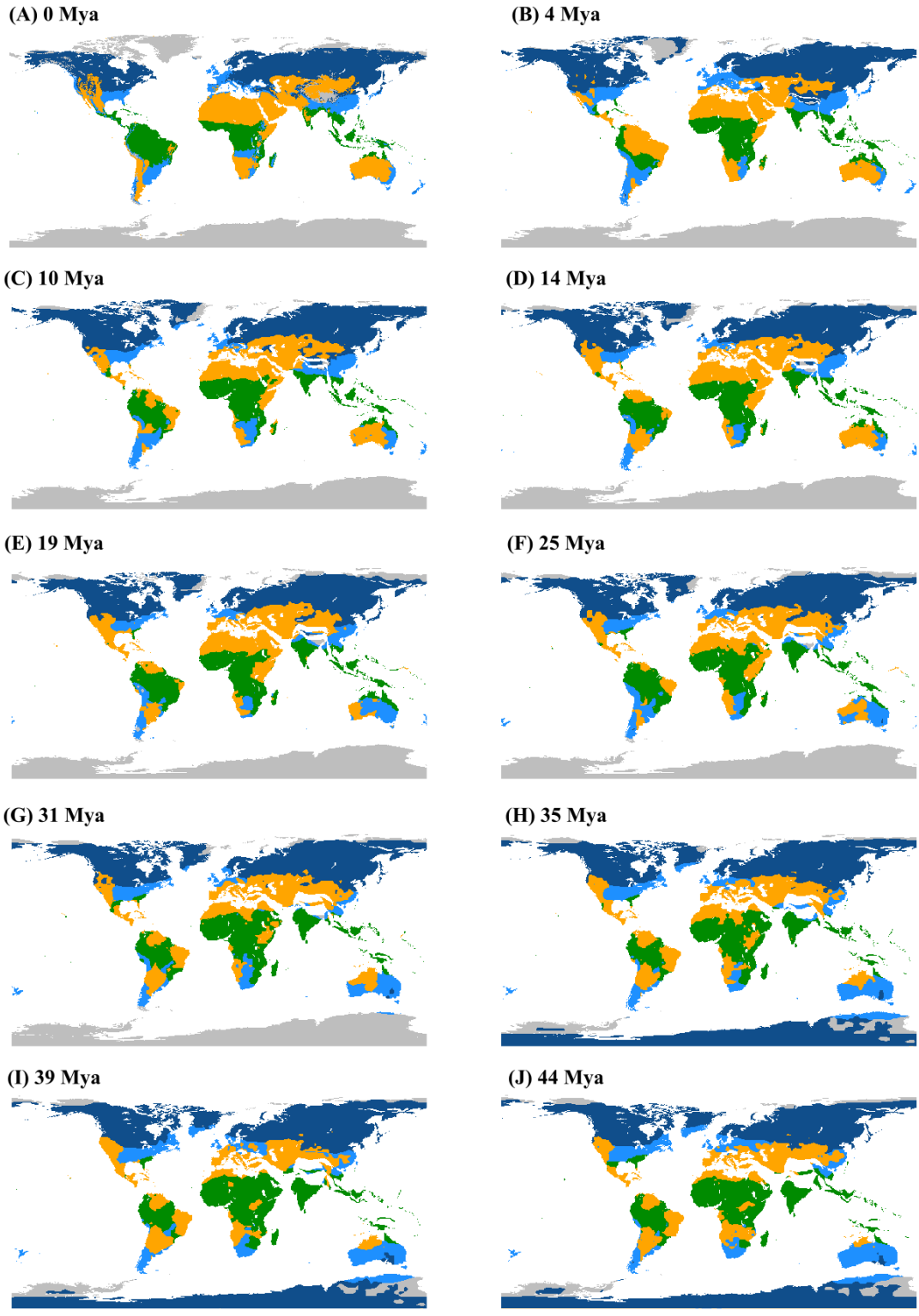
(A) 0 Mya
(B) 4 Mya
(C) 10 Mya
(D) 14 Mya
(E) 19 Mya
(F) 25 Mya
(G) 31 Mya
(H) 35 Mya
(I) 39 Mya
(J) 44 Mya
Koppen-Geiger main climate category
Tropical
Arid
Temperate
Cold
Polar

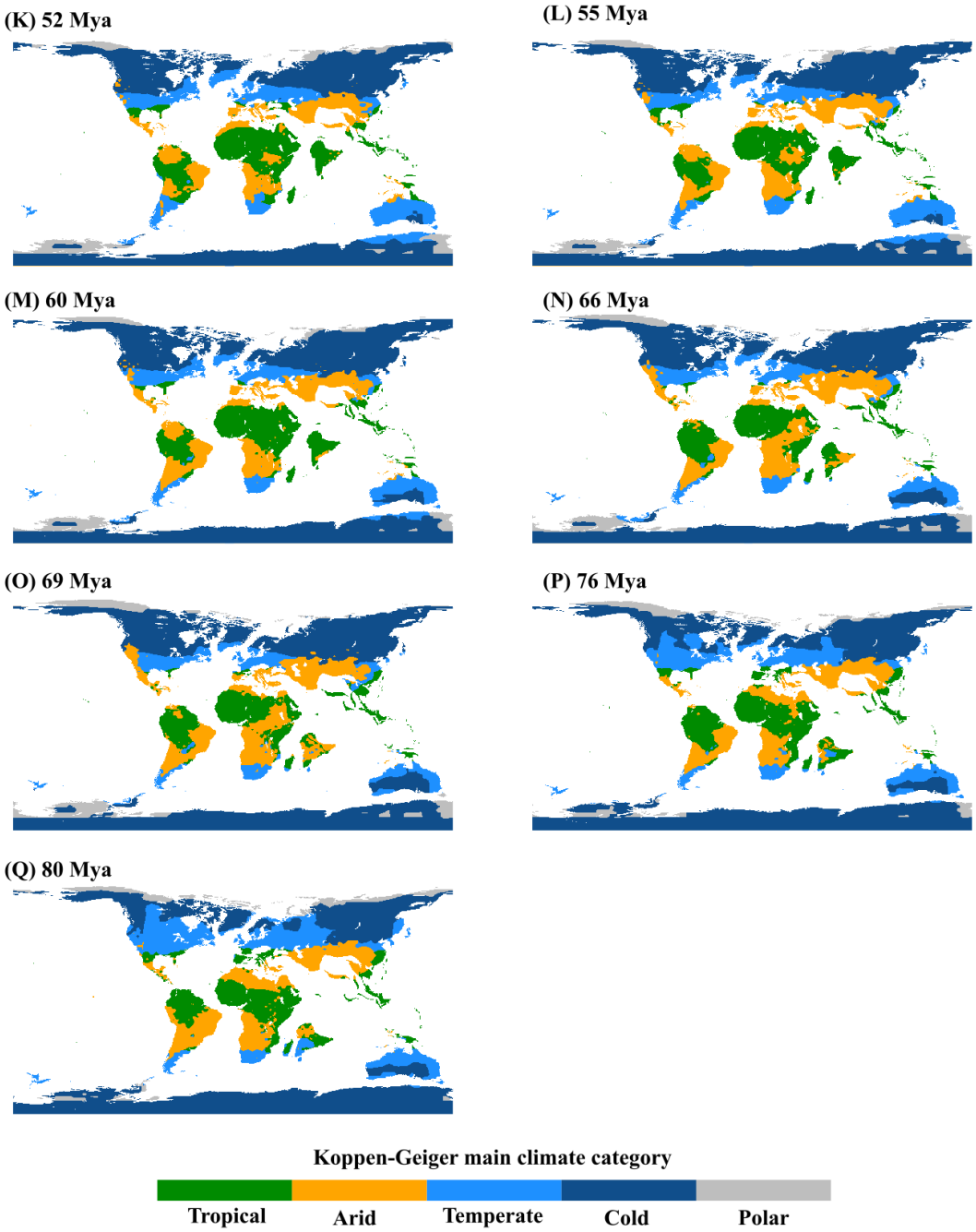

Fig. S7. Global Koppen-Geiger main climate reconstructions. (A), climates from the present were reconstructed using the WorldClim version 2 monthly data. (B-Q), all other paleo climates were reconstructed based on the simulated climate data from the HadCM3BL-M2.1aD general circulation model.

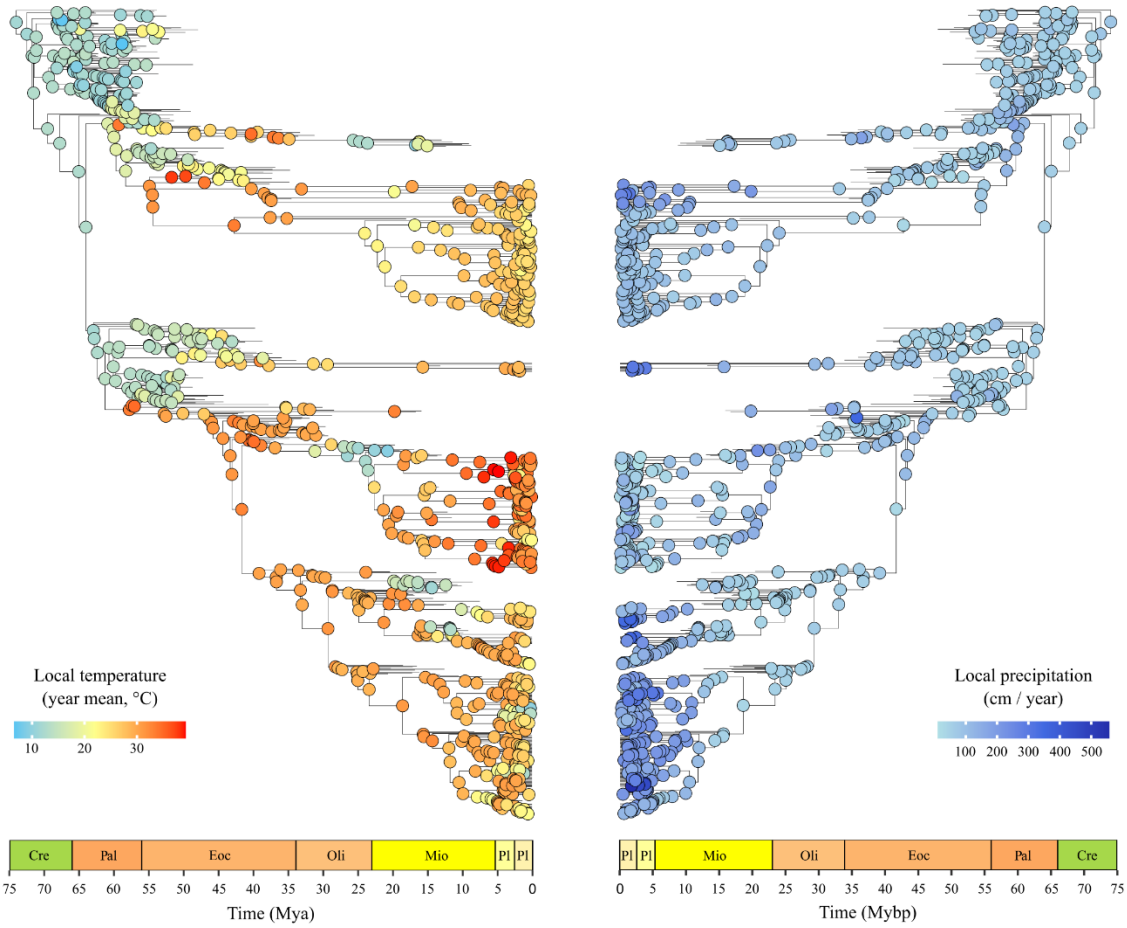

Fig. S8. Local precipitation and temperature extracted from ancestral locations at phylogenetic nodes. Values correspond to annual conditions, annual mean temperature and the total precipitation per year, respectively. These data were used to estimate the rate of change in local conditions (see Methods).

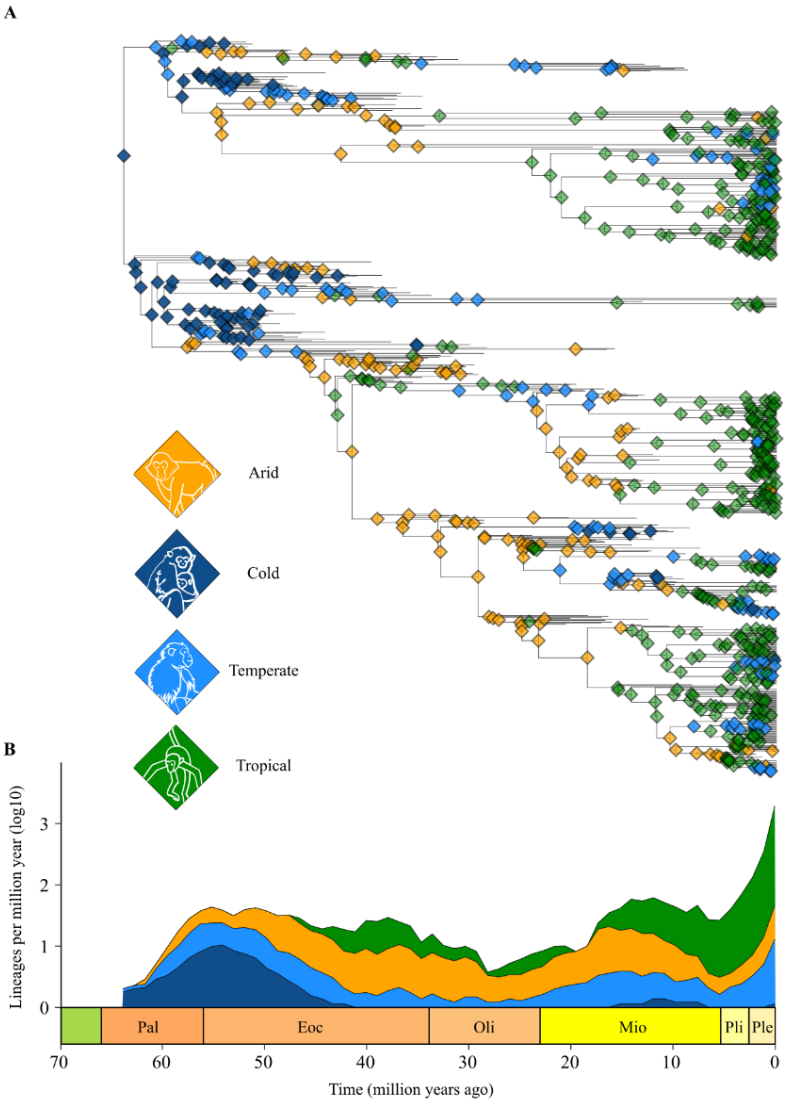

Fig. S9. Ancestral climates reconstructed with the Mk model for discrete trait evolution using the climates for extant and fossil tips as input data. (A), primates' phylogenetic tree with the Köppen-Geiger main climate categories identified for all nodes. We show the climate with the highest likelihood per node. (B), lineages through time intervals of one million years. Colors represent the relative proportion of lineages inhabiting each climate category. Please see Fig. 2 in the main text for comparison with ancestral climates reconstructed based on the Geo model and the GCM.

Table S1.

Geographic location of crown Primates inferred across a sample of 100 phylogenetic trees.

Sample Tree	Crown Euprimates Node Age	Restriction World Paleo Map Age	Median Posterior Longitude	Median Posterior Latitude	Paleo Continent
1	64.43	64	8.00	44.27	Europe
2	63.77	64	-79.34	51.99	North America
3	63.43	63	7.78	44.44	Europe
4	65.08	65	-77.04	52.44	North America
5	63.98	64	-78.90	52.81	North America
6	64.96	65	-78.30	52.46	North America
7	64.15	64	-80.13	52.13	North America
8	64.15	64	-77.87	52.42	North America
9	64.24	64	10.31	44.89	Europe
10	65.07	65	-78.92	52.09	North America
11	63.99	64	-79.71	52.33	North America
12	63.79	64	-79.39	52.14	North America
13	63.45	63	6.91	44.13	Europe
14	63.06	63	-80.15	51.98	North America
15	63.78	64	-79.34	51.83	North America
16	63.74	64	-80.31	51.82	North America
17	65.32	65	7.81	43.64	Europe
18	65.33	65	6.56	42.91	Europe
19	64.36	64	-78.28	52.70	North America
20	65.04	65	-79.70	51.88	North America
21	64.91	65	8.91	44.09	Europe
22	65.97	66	-79.18	52.11	North America
23	64.75	65	-78.42	52.05	North America
24	65.29	65	-78.72	51.94	North America
25	64.61	65	-79.02	52.01	North America
26	63.76	64	-79.37	51.99	North America
27	63.90	64	6.63	43.99	Europe

28	64.81	65	6.02	43.26	Europe
29	65.19	65	7.03	43.66	Europe
30	64.17	64	-80.15	52.26	North America
31	63.96	64	-78.74	52.22	North America
32	64.16	64	-79.50	51.84	North America
33	63.41	63	-76.63	52.47	North America
34	66.21	66	-77.83	52.15	North America
35	63.44	63	-77.61	52.90	North America
36	65.97	66	-79.69	52.32	North America
37	63.07	63	-78.37	51.98	North America
38	64.19	64	-75.57	51.78	North America
39	64.01	64	-78.83	52.11	North America
40	64.50	65	-77.42	53.74	North America
41	63.96	64	7.62	44.60	Europe
42	63.34	63	8.48	44.15	Europe
43	64.72	65	-78.54	52.14	North America
44	64.41	64	-78.36	51.67	North America
45	64.68	65	-79.51	52.15	North America
46	64.97	65	6.63	43.78	Europe
47	65.19	65	8.33	44.50	Europe
48	63.65	64	6.63	44.29	Europe
49	64.39	64	-78.92	52.29	North America
50	63.43	63	7.16	43.94	Europe
51	64.81	65	-79.06	51.81	North America
52	64.88	65	7.48	43.20	Europe
53	63.99	64	8.19	42.87	Europe
54	63.83	64	6.34	43.18	Europe
55	65.76	66	-79.92	52.14	North America
56	64.44	64	-79.41	51.94	North America
57	65.48	65	6.42	43.76	Europe
58	65.12	65	-76.12	52.53	North America

59	65.58	66	-77.65	52.41	North America
60	64.19	64	-77.43	52.40	North America
61	63.91	64	-74.99	52.92	North America
62	63.79	64	-80.47	52.00	North America
63	63.37	63	-77.69	52.44	North America
64	64.16	64	-78.99	52.42	North America
65	63.67	64	5.73	44.29	Europe
66	62.87	63	-75.84	52.40	North America
67	65.14	65	-80.18	52.07	North America
68	64.50	65	7.02	44.21	Europe
69	65.16	65	-78.48	51.93	North America
70	64.23	64	-79.66	52.32	North America
71	64.82	65	-79.15	52.11	North America
72	65.18	65	-77.57	52.36	North America
73	64.62	65	8.39	42.91	Europe
74	63.21	63	-79.52	52.27	North America
75	63.60	64	-78.22	51.61	North America
76	64.39	64	-79.70	51.77	North America
77	64.92	65	-12.93	58.96	Europe
78	63.22	63	6.52	44.30	Europe
79	65.62	66	-79.76	52.08	North America
80	64.84	65	-75.79	52.87	North America
81	65.06	65	6.05	43.10	Europe
82	63.87	64	6.35	44.30	Europe
83	64.03	64	-79.52	52.12	North America
84	64.15	64	-77.13	52.36	North America
85	64.52	65	-79.55	51.73	North America
86	64.65	65	-79.17	52.19	North America
87	65.36	65	9.54	43.85	Europe
88	63.71	64	3.15	42.79	Europe
89	64.49	64	-79.57	52.04	North America

90	64.46	64	-77.71	52.27	North America
91	64.07	64	-76.12	52.60	North America
92	64.54	65	-79.06	52.46	North America
93	65.14	65	-77.34	52.83	North America
94	65.11	65	-79.41	52.05	North America
95	63.35	63	-79.74	52.20	North America
96	65.02	65	-79.93	52.44	North America
97	64.37	64	-12.52	61.85	Europe
98	63.91	64	-79.68	52.18	North America
99	64.89	65	-79.09	52.25	North America
100	65.51	66	-79.07	52.22	North America

Table S2. Bayesian phylogenetic regression models predicting $D_{PATHWISE}$ and $NC_{PATHWISE}$ for Primates. Analyses are based on the median phylogenetic tree. The best-fit regression, given the marginal likelihood and deviance information criterion, for each response variable, is at the bottom. GT = Global temperature, LT = Local temperature, LT_{RATE} = Pathwise rate local temperature, LP = Local precipitation, LP_{RATE} = Pathwise rate local precipitation, DIC = Deviance information criterion, MLh = Marginal likelihood estimated by stepping-stones. Beta parameters in black are significant, i.e., PMCMC < 0.05. Beta parameters in grey-color are not significant, i.e., PMCMC > 0.05.

Response	**Predictors**	**DIC**	**MLh**	**R^2**
$D_{PATHWISE}$	$\beta_0 + \beta_1(Time) + \beta_2(GT)$	-	1448.32	0.07
	$\beta_0 + \beta_1(Time) + \beta_2(LT) + \beta_3(LP)$	-	1441.59	0.08
	$\beta_0 + \beta_1(Time) + \beta_2(LT) + \beta_3(LT_{RATE}) + \beta_4(LP_{RATE})$	-	1603.77	0.41
$NC_{PATHWISE}$	$\beta_0 + \beta_1(Time) + \beta_2(GT)$	4314.79	-	0.37
	$\beta_0 + \beta_1(Time) - \beta_2(LT) - \beta_3(LP)$	4313.48	-	0.37
	$\beta_0 + \beta_1(Time) - \beta_2(LT_{RATE}) + \beta_3(LP_{RATE})$	4290.25	-	0.50
	$\beta_0 + \beta_1(Time) + \beta_2(LP_{RATE})$	4289.05	-	0.49
	$\beta_0 + \beta_1(Time) – \beta_2(LT) – \beta_3(LP) + \beta_4(LP_{RATE})$	4281.92	-	0.51

Table S3.

Effect size of the variables affecting $D_{PATHWISE}$ and $NC_{PATHWISE}$. R^2_{DELTA} is the effect size of each variable. Effect size was calculated from the difference between the R^2 of the regression containing all significant variables and the R^2 of the regression excluding the variable in question.

Response	**Variable**	**P_{MCMC}**	**R^2_{DELTA}**
$D_{PATHWISE}$	Time	0.004	0.004
	LT	0	0.015
	LT_{RATE}	0	0.19
	LP_{RATE}	0	0.021
$NC_{PATHWISE}$	Time	0.02	0.001
	LT	0.04	0.001
	LP	0.004	0.02
	LP_{RATE}	0	0.14

Table S4.

Phylogenetic regression predicting $D_{PATHWISE}$ across the sample of 100 phylogenetic trees of Primates. Beta parameters in black are significant, i.e., $P_{MCMC} < 0.05$. Beta parameters in grey are not significant, i.e., $P_{MCMC} > 0.05$.

Sample tree	Response	Predictors	R^2
1	$D_{PATHWISE}$	$\beta_0 + \beta_1(Time) + \beta_2(GT) + \beta_3(LT) + \beta_4(LP) + \beta_5(LT_{RATE}) + \beta_6(LP_{RATE})$	0.40
2	$D_{PATHWISE}$	$\beta_0 + \beta_1(Time) + \beta_2(GT) + \beta_3(LT) + \beta_4(LP) + \beta_5(LT_{RATE}) + \beta_6(LP_{RATE})$	0.67
3	$D_{PATHWISE}$	$\beta_0 + \beta_1(Time) + \beta_2(GT) + \beta_3(LT) + \beta_4(LP) + \beta_5(LT_{RATE}) + \beta_6(LP_{RATE})$	0.43
4	$D_{PATHWISE}$	$\beta_0 + \beta_1(Time) + \beta_2(GT) + \beta_3(LT) + \beta_4(LP) + \beta_5(LT_{RATE}) + \beta_6(LP_{RATE})$	0.51
5	$D_{PATHWISE}$	$\beta_0 + \beta_1(Time) + \beta_2(GT) + \beta_3(LT) + \beta_4(LP) + \beta_5(LT_{RATE}) + \beta_6(LP_{RATE})$	0.59
6	$D_{PATHWISE}$	$\beta_0 + \beta_1(Time) + \beta_2(GT) + \beta_3(LT) + \beta_4(LP) + \beta_5(LT_{RATE}) + \beta_6(LP_{RATE})$	0.71
7	$D_{PATHWISE}$	$\beta_0 + \beta_1(Time) + \beta_2(GT) + \beta_3(LT) + \beta_4(LP) + \beta_5(LT_{RATE}) + \beta_6(LP_{RATE})$	0.48
8	$D_{PATHWISE}$	$\beta_0 + \beta_1(Time) + \beta_2(GT) + \beta_3(LT) + \beta_4(LP) + \beta_5(LT_{RATE}) + \beta_6(LP_{RATE})$	0.67
9	$D_{PATHWISE}$	$\beta_0 + \beta_1(Time) + \beta_2(GT) + \beta_3(LT) + \beta_4(LP) + \beta_5(LT_{RATE}) + \beta_6(LP_{RATE})$	0.38
10	$D_{PATHWISE}$	$\beta_0 + \beta_1(Time) + \beta_2(GT) + \beta_3(LT) + \beta_4(LP) + \beta_5(LT_{RATE}) + \beta_6(LP_{RATE})$	0.62
11	$D_{PATHWISE}$	$\beta_0 + \beta_1(Time) + \beta_2(GT) + \beta_3(LT) + \beta_4(LP) + \beta_5(LT_{RATE}) + \beta_6(LP_{RATE})$	0.61
12	$D_{PATHWISE}$	$\beta_0 + \beta_1(Time) + \beta_2(GT) + \beta_3(LT) + \beta_4(LP) + \beta_5(LT_{RATE}) + \beta_6(LP_{RATE})$	0.63
13	$D_{PATHWISE}$	$\beta_0 + \beta_1(Time) + \beta_2(GT) + \beta_3(LT) + \beta_4(LP) + \beta_5(LT_{RATE}) + \beta_6(LP_{RATE})$	0.39
14	$D_{PATHWISE}$	$\beta_0 + \beta_1(Time) + \beta_2(GT) + \beta_3(LT) + \beta_4(LP) + \beta_5(LT_{RATE}) + \beta_6(LP_{RATE})$	0.65
15	$D_{PATHWISE}$	$\beta_0 + \beta_1(Time) + \beta_2(GT) + \beta_3(LT) + \beta_4(LP) + \beta_5(LT_{RATE}) + \beta_6(LP_{RATE})$	0.64
16	$D_{PATHWISE}$	$\beta_0 + \beta_1(Time) + \beta_2(GT) + \beta_3(LT) + \beta_4(LP) + \beta_5(LT_{RATE}) + \beta_6(LP_{RATE})$	0.56
17	$D_{PATHWISE}$	$\beta_0 + \beta_1(Time) + \beta_2(GT) + \beta_3(LT) + \beta_4(LP) + \beta_5(LT_{RATE}) + \beta_6(LP_{RATE})$	0.43
18	$D_{PATHWISE}$	$\beta_0 + \beta_1(Time) + \beta_2(GT) + \beta_3(LT) + \beta_4(LP) + \beta_5(LT_{RATE}) + \beta_6(LP_{RATE})$	0.41
19	$D_{PATHWISE}$	$\beta_0 + \beta_1(Time) + \beta_2(GT) + \beta_3(LT) + \beta_4(LP) + \beta_5(LT_{RATE}) + \beta_6(LP_{RATE})$	0.67
20	$D_{PATHWISE}$	$\beta_0 + \beta_1(Time) + \beta_2(GT) + \beta_3(LT) + \beta_4(LP) + \beta_5(LT_{RATE}) + \beta_6(LP_{RATE})$	0.64
21	$D_{PATHWISE}$	$\beta_0 + \beta_1(Time) + \beta_2(GT) + \beta_3(LT) + \beta_4(LP) + \beta_5(LT_{RATE}) + \beta_6(LP_{RATE})$	0.41
22	$D_{PATHWISE}$	$\beta_0 + \beta_1(Time) + \beta_2(GT) + \beta_3(LT) + \beta_4(LP) + \beta_5(LT_{RATE}) + \beta_6(LP_{RATE})$	0.55
23	$D_{PATHWISE}$	$\beta_0 + \beta_1(Time) + \beta_2(GT) + \beta_3(LT) + \beta_4(LP) + \beta_5(LT_{RATE}) + \beta_6(LP_{RATE})$	0.59
24	$D_{PATHWISE}$	$\beta_0 + \beta_1(Time) + \beta_2(GT) + \beta_3(LT) + \beta_4(LP) + \beta_5(LT_{RATE}) + \beta_6(LP_{RATE})$	0.57
25	$D_{PATHWISE}$	$\beta_0 + \beta_1(Time) + \beta_2(GT) + \beta_3(LT) + \beta_4(LP) + \beta_5(LT_{RATE}) + \beta_6(LP_{RATE})$	0.69
26	$D_{PATHWISE}$	$\beta_0 + \beta_1(Time) + \beta_2(GT) + \beta_3(LT) + \beta_4(LP) + \beta_5(LT_{RATE}) + \beta_6(LP_{RATE})$	0.63
27	$D_{PATHWISE}$	$\beta_0 + \beta_1(Time) + \beta_2(GT) + \beta_3(LT) + \beta_4(LP) + \beta_5(LT_{RATE}) + \beta_6(LP_{RATE})$	0.41

28	$D_{PATHWISE}$	$\beta_0 + \beta_1(Time) + \beta_2(GT) + \beta_3(LT) + \beta_4(LP) + \beta_5(LT_{RATE}) + \beta_6(LP_{RATE})$	0.47
29	$D_{PATHWISE}$	$\beta_0 + \beta_1(Time) + \beta_2(GT) + \beta_3(LT) + \beta_4(LP) + \beta_5(LT_{RATE}) + \beta_6(LP_{RATE})$	0.57
30	$D_{PATHWISE}$	$\beta_0 + \beta_1(Time) + \beta_2(GT) + \beta_3(LT) + \beta_4(LP) + \beta_5(LT_{RATE}) + \beta_6(LP_{RATE})$	0.54
31	$D_{PATHWISE}$	$\beta_0 + \beta_1(Time) + \beta_2(GT) + \beta_3(LT) + \beta_4(LP) + \beta_5(LT_{RATE}) + \beta_6(LP_{RATE})$	0.59
32	$D_{PATHWISE}$	$\beta_0 + \beta_1(Time) + \beta_2(GT) + \beta_3(LT) + \beta_4(LP) + \beta_5(LT_{RATE}) + \beta_6(LP_{RATE})$	0.62
33	$D_{PATHWISE}$	$\beta_0 + \beta_1(Time) + \beta_2(GT) + \beta_3(LT) + \beta_4(LP) + \beta_5(LT_{RATE}) + \beta_6(LP_{RATE})$	0.63
34	$D_{PATHWISE}$	$\beta_0 + \beta_1(Time) + \beta_2(GT) + \beta_3(LT) + \beta_4(LP) + \beta_5(LT_{RATE}) + \beta_6(LP_{RATE})$	0.55
35	$D_{PATHWISE}$	$\beta_0 + \beta_1(Time) + \beta_2(GT) + \beta_3(LT) + \beta_4(LP) + \beta_5(LT_{RATE}) + \beta_6(LP_{RATE})$	0.59
36	$D_{PATHWISE}$	$\beta_0 + \beta_1(Time) + \beta_2(GT) + \beta_3(LT) + \beta_4(LP) + \beta_5(LT_{RATE}) + \beta_6(LP_{RATE})$	0.59
37	$D_{PATHWISE}$	$\beta_0 + \beta_1(Time) + \beta_2(GT) + \beta_3(LT) + \beta_4(LP) + \beta_5(LT_{RATE}) + \beta_6(LP_{RATE})$	0.44
38	$D_{PATHWISE}$	$\beta_0 + \beta_1(Time) + \beta_2(GT) + \beta_3(LT) + \beta_4(LP) + \beta_5(LT_{RATE}) + \beta_6(LP_{RATE})$	0.60
39	$D_{PATHWISE}$	$\beta_0 + \beta_1(Time) + \beta_2(GT) + \beta_3(LT) + \beta_4(LP) + \beta_5(LT_{RATE}) + \beta_6(LP_{RATE})$	0.48
40	$D_{PATHWISE}$	$\beta_0 + \beta_1(Time) + \beta_2(GT) + \beta_3(LT) + \beta_4(LP) + \beta_5(LT_{RATE}) + \beta_6(LP_{RATE})$	0.51
41	$D_{PATHWISE}$	$\beta_0 + \beta_1(Time) + \beta_2(GT) + \beta_3(LT) + \beta_4(LP) + \beta_5(LT_{RATE}) + \beta_6(LP_{RATE})$	0.37
42	$D_{PATHWISE}$	$\beta_0 + \beta_1(Time) + \beta_2(GT) + \beta_3(LT) + \beta_4(LP) + \beta_5(LT_{RATE}) + \beta_6(LP_{RATE})$	0.51
43	$D_{PATHWISE}$	$\beta_0 + \beta_1(Time) + \beta_2(GT) + \beta_3(LT) + \beta_4(LP) + \beta_5(LT_{RATE}) + \beta_6(LP_{RATE})$	0.52
44	$D_{PATHWISE}$	$\beta_0 + \beta_1(Time) + \beta_2(GT) + \beta_3(LT) + \beta_4(LP) + \beta_5(LT_{RATE}) + \beta_6(LP_{RATE})$	0.64
45	$D_{PATHWISE}$	$\beta_0 + \beta_1(Time) + \beta_2(GT) + \beta_3(LT) + \beta_4(LP) + \beta_5(LT_{RATE}) + \beta_6(LP_{RATE})$	0.61
46	$D_{PATHWISE}$	$\beta_0 + \beta_1(Time) + \beta_2(GT) + \beta_3(LT) + \beta_4(LP) + \beta_5(LT_{RATE}) + \beta_6(LP_{RATE})$	0.45
47	$D_{PATHWISE}$	$\beta_0 + \beta_1(Time) + \beta_2(GT) + \beta_3(LT) + \beta_4(LP) + \beta_5(LT_{RATE}) + \beta_6(LP_{RATE})$	0.41
48	$D_{PATHWISE}$	$\beta_0 + \beta_1(Time) + \beta_2(GT) + \beta_3(LT) + \beta_4(LP) + \beta_5(LT_{RATE}) + \beta_6(LP_{RATE})$	0.57
49	$D_{PATHWISE}$	$\beta_0 + \beta_1(Time) + \beta_2(GT) + \beta_3(LT) + \beta_4(LP) + \beta_5(LT_{RATE}) + \beta_6(LP_{RATE})$	0.64
50	$D_{PATHWISE}$	$\beta_0 + \beta_1(Time) + \beta_2(GT) + \beta_3(LT) + \beta_4(LP) + \beta_5(LT_{RATE}) + \beta_6(LP_{RATE})$	0.42
51	$D_{PATHWISE}$	$\beta_0 + \beta_1(Time) + \beta_2(GT) + \beta_3(LT) + \beta_4(LP) + \beta_5(LT_{RATE}) + \beta_6(LP_{RATE})$	0.66
52	$D_{PATHWISE}$	$\beta_0 + \beta_1(Time) + \beta_2(GT) + \beta_3(LT) + \beta_4(LP) + \beta_5(LT_{RATE}) + \beta_6(LP_{RATE})$	0.47
53	$D_{PATHWISE}$	$\beta_0 + \beta_1(Time) + \beta_2(GT) + \beta_3(LT) + \beta_4(LP) + \beta_5(LT_{RATE}) + \beta_6(LP_{RATE})$	0.46
54	$D_{PATHWISE}$	$\beta_0 + \beta_1(Time) + \beta_2(GT) + \beta_3(LT) + \beta_4(LP) + \beta_5(LT_{RATE}) + \beta_6(LP_{RATE})$	0.45
55	$D_{PATHWISE}$	$\beta_0 + \beta_1(Time) + \beta_2(GT) + \beta_3(LT) + \beta_4(LP) + \beta_5(LT_{RATE}) + \beta_6(LP_{RATE})$	0.58
56	$D_{PATHWISE}$	$\beta_0 + \beta_1(Time) + \beta_2(GT) + \beta_3(LT) + \beta_4(LP) + \beta_5(LT_{RATE}) + \beta_6(LP_{RATE})$	0.61
57	$D_{PATHWISE}$	$\beta_0 + \beta_1(Time) + \beta_2(GT) + \beta_3(LT) + \beta_4(LP) + \beta_5(LT_{RATE}) + \beta_6(LP_{RATE})$	0.40
58	$D_{PATHWISE}$	$\beta_0 + \beta_1(Time) + \beta_2(GT) + \beta_3(LT) + \beta_4(LP) + \beta_5(LT_{RATE}) + \beta_6(LP_{RATE})$	0.57

59	$D_{PATHWISE}$	$\beta_0 + \beta_1(Time) + \beta_2(GT) + \beta_3(LT) + \beta_4(LP) + \beta_5(LT_{RATE}) + \beta_6(LP_{RATE})$	0.60
60	$D_{PATHWISE}$	$\beta_0 + \beta_1(Time) + \beta_2(GT) + \beta_3(LT) + \beta_4(LP) + \beta_5(LT_{RATE}) + \beta_6(LP_{RATE})$	0.51
61	$D_{PATHWISE}$	$\beta_0 + \beta_1(Time) + \beta_2(GT) + \beta_3(LT) + \beta_4(LP) + \beta_5(LT_{RATE}) + \beta_6(LP_{RATE})$	0.45
62	$D_{PATHWISE}$	$\beta_0 + \beta_1(Time) + \beta_2(GT) + \beta_3(LT) + \beta_4(LP) + \beta_5(LT_{RATE}) + \beta_6(LP_{RATE})$	0.58
63	$D_{PATHWISE}$	$\beta_0 + \beta_1(Time) + \beta_2(GT) + \beta_3(LT) + \beta_4(LP) + \beta_5(LT_{RATE}) + \beta_6(LP_{RATE})$	0.52
64	$D_{PATHWISE}$	$\beta_0 + \beta_1(Time) + \beta_2(GT) + \beta_3(LT) + \beta_4(LP) + \beta_5(LT_{RATE}) + \beta_6(LP_{RATE})$	0.60
65	$D_{PATHWISE}$	$\beta_0 + \beta_1(Time) + \beta_2(GT) + \beta_3(LT) + \beta_4(LP) + \beta_5(LT_{RATE}) + \beta_6(LP_{RATE})$	0.51
66	$D_{PATHWISE}$	$\beta_0 + \beta_1(Time) + \beta_2(GT) + \beta_3(LT) + \beta_4(LP) + \beta_5(LT_{RATE}) + \beta_6(LP_{RATE})$	0.59
67	$D_{PATHWISE}$	$\beta_0 + \beta_1(Time) + \beta_2(GT) + \beta_3(LT) + \beta_4(LP) + \beta_5(LT_{RATE}) + \beta_6(LP_{RATE})$	0.54
68	$D_{PATHWISE}$	$\beta_0 + \beta_1(Time) + \beta_2(GT) + \beta_3(LT) + \beta_4(LP) + \beta_5(LT_{RATE}) + \beta_6(LP_{RATE})$	0.43
69	$D_{PATHWISE}$	$\beta_0 + \beta_1(Time) + \beta_2(GT) + \beta_3(LT) + \beta_4(LP) + \beta_5(LT_{RATE}) + \beta_6(LP_{RATE})$	0.63
70	$D_{PATHWISE}$	$\beta_0 + \beta_1(Time) + \beta_2(GT) + \beta_3(LT) + \beta_4(LP) + \beta_5(LT_{RATE}) + \beta_6(LP_{RATE})$	0.59
71	$D_{PATHWISE}$	$\beta_0 + \beta_1(Time) + \beta_2(GT) + \beta_3(LT) + \beta_4(LP) + \beta_5(LT_{RATE}) + \beta_6(LP_{RATE})$	0.59
72	$D_{PATHWISE}$	$\beta_0 + \beta_1(Time) + \beta_2(GT) + \beta_3(LT) + \beta_4(LP) + \beta_5(LT_{RATE}) + \beta_6(LP_{RATE})$	0.54
73	$D_{PATHWISE}$	$\beta_0 + \beta_1(Time) + \beta_2(GT) + \beta_3(LT) + \beta_4(LP) + \beta_5(LT_{RATE}) + \beta_6(LP_{RATE})$	0.47
74	$D_{PATHWISE}$	$\beta_0 + \beta_1(Time) + \beta_2(GT) + \beta_3(LT) + \beta_4(LP) + \beta_5(LT_{RATE}) + \beta_6(LP_{RATE})$	0.60
75	$D_{PATHWISE}$	$\beta_0 + \beta_1(Time) + \beta_2(GT) + \beta_3(LT) + \beta_4(LP) + \beta_5(LT_{RATE}) + \beta_6(LP_{RATE})$	0.64
76	$D_{PATHWISE}$	$\beta_0 + \beta_1(Time) + \beta_2(GT) + \beta_3(LT) + \beta_4(LP) + \beta_5(LT_{RATE}) + \beta_6(LP_{RATE})$	0.64
77	$D_{PATHWISE}$	$\beta_0 + \beta_1(Time) + \beta_2(GT) + \beta_3(LT) + \beta_4(LP) + \beta_5(LT_{RATE}) + \beta_6(LP_{RATE})$	0.44
78	$D_{PATHWISE}$	$\beta_0 + \beta_1(Time) + \beta_2(GT) + \beta_3(LT) + \beta_4(LP) + \beta_5(LT_{RATE}) + \beta_6(LP_{RATE})$	0.49
79	$D_{PATHWISE}$	$\beta_0 + \beta_1(Time) + \beta_2(GT) + \beta_3(LT) + \beta_4(LP) + \beta_5(LT_{RATE}) + \beta_6(LP_{RATE})$	0.63
80	$D_{PATHWISE}$	$\beta_0 + \beta_1(Time) + \beta_2(GT) + \beta_3(LT) + \beta_4(LP) + \beta_5(LT_{RATE}) + \beta_6(LP_{RATE})$	0.52
81	$D_{PATHWISE}$	$\beta_0 + \beta_1(Time) + \beta_2(GT) + \beta_3(LT) + \beta_4(LP) + \beta_5(LT_{RATE}) + \beta_6(LP_{RATE})$	0.59
82	$D_{PATHWISE}$	$\beta_0 + \beta_1(Time) + \beta_2(GT) + \beta_3(LT) + \beta_4(LP) + \beta_5(LT_{RATE}) + \beta_6(LP_{RATE})$	0.50
83	$D_{PATHWISE}$	$\beta_0 + \beta_1(Time) + \beta_2(GT) + \beta_3(LT) + \beta_4(LP) + \beta_5(LT_{RATE}) + \beta_6(LP_{RATE})$	0.56
84	$D_{PATHWISE}$	$\beta_0 + \beta_1(Time) + \beta_2(GT) + \beta_3(LT) + \beta_4(LP) + \beta_5(LT_{RATE}) + \beta_6(LP_{RATE})$	0.57
85	$D_{PATHWISE}$	$\beta_0 + \beta_1(Time) + \beta_2(GT) + \beta_3(LT) + \beta_4(LP) + \beta_5(LT_{RATE}) + \beta_6(LP_{RATE})$	0.61
86	$D_{PATHWISE}$	$\beta_0 + \beta_1(Time) + \beta_2(GT) + \beta_3(LT) + \beta_4(LP) + \beta_5(LT_{RATE}) + \beta_6(LP_{RATE})$	0.63
87	$D_{PATHWISE}$	$\beta_0 + \beta_1(Time) + \beta_2(GT) + \beta_3(LT) + \beta_4(LP) + \beta_5(LT_{RATE}) + \beta_6(LP_{RATE})$	0.46
88	$D_{PATHWISE}$	$\beta_0 + \beta_1(Time) + \beta_2(GT) + \beta_3(LT) + \beta_4(LP) + \beta_5(LT_{RATE}) + \beta_6(LP_{RATE})$	0.46
89	$D_{PATHWISE}$	$\beta_0 + \beta_1(Time) + \beta_2(GT) + \beta_3(LT) + \beta_4(LP) + \beta_5(LT_{RATE}) + \beta_6(LP_{RATE})$	0.60

90	$D_{PATHWISE}$	$\beta_0 + \beta_1(\text{Time}) + \beta_2(\text{GT}) + \beta_3(\text{LT}) + \beta_4(\text{LP}) + \beta_5(LT_{RATE}) + \beta_6(LP_{RATE})$	0.63
91	$D_{PATHWISE}$	$\beta_0 + \beta_1(\text{Time}) + \beta_2(\text{GT}) + \beta_3(\text{LT}) + \beta_4(\text{LP}) + \beta_5(LT_{RATE}) + \beta_6(LP_{RATE})$	0.59
92	$D_{PATHWISE}$	$\beta_0 + \beta_1(\text{Time}) + \beta_2(\text{GT}) + \beta_3(\text{LT}) + \beta_4(\text{LP}) + \beta_5(LT_{RATE}) + \beta_6(LP_{RATE})$	0.63
93	$D_{PATHWISE}$	$\beta_0 + \beta_1(\text{Time}) + \beta_2(\text{GT}) + \beta_3(\text{LT}) + \beta_4(\text{LP}) + \beta_5(LT_{RATE}) + \beta_6(LP_{RATE})$	0.54
94	$D_{PATHWISE}$	$\beta_0 + \beta_1(\text{Time}) + \beta_2(\text{GT}) + \beta_3(\text{LT}) + \beta_4(\text{LP}) + \beta_5(LT_{RATE}) + \beta_6(LP_{RATE})$	0.60
95	$D_{PATHWISE}$	$\beta_0 + \beta_1(\text{Time}) + \beta_2(\text{GT}) + \beta_3(\text{LT}) + \beta_4(\text{LP}) + \beta_5(LT_{RATE}) + \beta_6(LP_{RATE})$	0.60
96	$D_{PATHWISE}$	$\beta_0 + \beta_1(\text{Time}) + \beta_2(\text{GT}) + \beta_3(\text{LT}) + \beta_4(\text{LP}) + \beta_5(LT_{RATE}) + \beta_6(LP_{RATE})$	0.58
97	$D_{PATHWISE}$	$\beta_0 + \beta_1(\text{Time}) + \beta_2(\text{GT}) + \beta_3(\text{LT}) + \beta_4(\text{LP}) + \beta_5(LT_{RATE}) + \beta_6(LP_{RATE})$	0.46
98	$D_{PATHWISE}$	$\beta_0 + \beta_1(\text{Time}) + \beta_2(\text{GT}) + \beta_3(\text{LT}) + \beta_4(\text{LP}) + \beta_5(LT_{RATE}) + \beta_6(LP_{RATE})$	0.61
99	$D_{PATHWISE}$	$\beta_0 + \beta_1(\text{Time}) + \beta_2(\text{GT}) + \beta_3(\text{LT}) + \beta_4(\text{LP}) + \beta_5(LT_{RATE}) + \beta_6(LP_{RATE})$	0.61
100	$D_{PATHWISE}$	$\beta_0 + \beta_1(\text{Time}) + \beta_2(\text{GT}) + \beta_3(\text{LT}) + \beta_4(\text{LP}) + \beta_5(LT_{RATE}) + \beta_6(LP_{RATE})$	0.65

Table S5.

Phylogenetic regression predicting $NC_{PATHWISE}$ across the sample of 100 phylogenetic trees of Primates. $P_{MCMC} < 0.05$ indicates predictor statistically significant effect.

Sample Tree	P_{MCMC} Intercept	P_{MCMC} Time	P_{MCMC} GT	P_{MCMC} LT	P_{MCMC} LP	P_{MCMC} LT_{RATE}	P_{MCMC} LP_{RATE}	R^2
1	0.001	0.002	0.112	0.046	0.026	0.894	0.001	0.54
2	0.001	0.001	0.236	0.052	0.008	0.026	0.001	0.45
3	0.004	0.002	0.102	0.196	0.004	0.574	0.001	0.55
4	0.001	0.001	0.498	0.19	0.012	0.248	0.001	0.42
5	0.001	0.001	0.18	0.072	0.002	0.11	0.001	0.45
6	0.001	0.001	0.19	0.05	0.01	0.124	0.001	0.45
7	0.001	0.001	0.136	0.058	0.016	0.462	0.001	0.45
8	0.001	0.001	0.152	0.042	0.016	0.35	0.001	0.47
9	0.001	0.001	0.1	0.112	0.006	0.486	0.001	0.57
10	0.001	0.001	0.13	0.062	0.014	0.37	0.002	0.42
11	0.001	0.001	0.178	0.034	0.012	0.384	0.001	0.47
12	0.001	0.002	0.246	0.022	0.02	0.086	0.001	0.43
13	0.001	0.006	0.164	0.096	0.006	0.548	0.001	0.52
14	0.001	0.01	0.582	0.062	0.014	0.028	0.001	0.41
15	0.001	0.001	0.038	0.072	0.01	0.358	0.001	0.49
16	0.001	0.004	0.194	0.142	0.006	0.604	0.001	0.43
17	0.004	0.002	0.094	0.096	0.016	0.842	0.001	0.53
18	0.001	0.004	0.266	0.138	0.001	0.79	0.001	0.46
19	0.001	0.001	0.314	0.052	0.004	0.12	0.001	0.43
20	0.001	0.001	0.102	0.034	0.02	0.76	0.001	0.47
21	0.001	0.004	0.15	0.04	0.001	0.972	0.001	0.55
22	0.001	0.001	0.13	0.088	0.016	0.544	0.001	0.48
23	0.001	0.004	0.222	0.066	0.02	0.3	0.001	0.44
24	0.001	0.001	0.23	0.122	0.028	0.72	0.001	0.41
25	0.001	0.002	0.218	0.056	0.016	0.012	0.001	0.45
26	0.001	0.001	0.098	0.052	0.058	0.506	0.001	0.51
27	0.001	0.004	0.254	0.068	0.001	0.724	0.001	0.52

28	0.001	0.002	0.09	0.07	0.008	0.76	0.001	0.52
29	0.016	0.002	0.02	0.066	0.014	0.818	0.001	0.54
30	0.004	0.006	0.142	0.064	0.006	0.858	0.001	0.51
31	0.001	0.001	0.18	0.104	0.03	0.26	0.001	0.44
32	0.001	0.001	0.29	0.072	0.006	0.03	0.001	0.42
33	0.001	0.006	0.434	0.038	0.014	0.098	0.001	0.44
34	0.001	0.001	0.196	0.134	0.026	0.84	0.001	0.47
35	0.001	0.001	0.278	0.164	0.004	0.25	0.001	0.42
36	0.001	0.004	0.37	0.06	0.014	0.24	0.001	0.48
37	0.001	0.001	0.21	0.042	0.008	0.126	0.001	0.44
38	0.001	0.002	0.196	0.058	0.018	0.232	0.001	0.47
39	0.001	0.001	0.58	0.098	0.062	0.72	0.016	0.43
40	0.001	0.004	0.306	0.082	0.02	0.718	0.001	0.45
41	0.001	0.006	0.066	0.142	0.004	0.326	0.001	0.58
42	0.001	0.004	0.224	0.186	0.002	0.92	0.001	0.46
43	0.001	0.001	0.128	0.04	0.034	0.734	0.001	0.44
44	0.001	0.004	0.248	0.014	0.01	0.076	0.001	0.46
45	0.001	0.001	0.118	0.036	0.012	0.234	0.001	0.48
46	0.001	0.004	0.176	0.034	0.004	0.408	0.001	0.56
47	0.001	0.008	0.132	0.09	0.004	0.78	0.001	0.52
48	0.002	0.004	0.136	0.048	0.028	0.948	0.001	0.60
49	0.001	0.001	0.152	0.064	0.036	0.722	0.001	0.45
50	0.001	0.006	0.286	0.042	0.002	0.48	0.001	0.53
51	0.001	0.001	0.188	0.022	0.016	0.054	0.001	0.50
52	0.001	0.004	0.148	0.08	0.006	0.786	0.001	0.49
53	0.001	0.001	0.08	0.132	0.008	0.288	0.002	0.53
54	0.002	0.014	0.108	0.056	0.006	0.844	0.001	0.53
55	0.001	0.001	0.276	0.082	0.014	0.184	0.001	0.44
56	0.001	0.001	0.194	0.008	0.004	0.036	0.001	0.47
57	0.001	0.016	0.152	0.076	0.001	0.804	0.001	0.52
58	0.001	0.002	0.26	0.054	0.024	0.37	0.001	0.47

59	0.001	0.004	0.082	0.054	0.026	0.39	0.001	0.46
60	0.001	0.006	0.21	0.078	0.018	0.648	0.001	0.45
61	0.001	0.001	0.21	0.104	0.018	0.396	0.001	0.46
62	0.001	0.001	0.202	0.056	0.012	0.06	0.001	0.46
63	0.001	0.001	0.248	0.136	0.038	0.556	0.001	0.45
64	0.001	0.001	0.358	0.06	0.016	0.24	0.001	0.43
65	0.001	0.001	0.222	0.08	0.004	0.374	0.001	0.49
66	0.001	0.008	0.498	0.104	0.012	0.574	0.001	0.44
67	0.001	0.001	0.182	0.038	0.016	0.432	0.001	0.42
68	0.002	0.001	0.124	0.166	0.012	0.754	0.001	0.51
69	0.001	0.002	0.362	0.146	0.026	0.476	0.001	0.39
70	0.001	0.001	0.252	0.07	0.036	0.258	0.001	0.45
71	0.001	0.001	0.218	0.098	0.032	0.424	0.001	0.44
72	0.001	0.002	0.242	0.086	0.04	0.432	0.001	0.45
73	0.001	0.008	0.108	0.12	0.002	0.99	0.001	0.49
74	0.001	0.001	0.166	0.02	0.012	0.378	0.001	0.47
75	0.001	0.001	0.228	0.08	0.004	0.094	0.001	0.41
76	0.001	0.001	0.244	0.054	0.008	0.286	0.001	0.44
77	0.002	0.048	0.498	0.1	0.001	0.608	0.001	0.53
78	0.001	0.006	0.098	0.102	0.01	0.928	0.001	0.50
79	0.001	0.002	0.234	0.054	0.014	0.454	0.001	0.46
80	0.001	0.001	0.222	0.054	0.008	0.628	0.001	0.47
81	0.014	0.006	0.092	0.094	0.008	0.35	0.001	0.53
82	0.001	0.008	0.324	0.12	0.014	0.978	0.001	0.45
83	0.001	0.001	0.062	0.064	0.06	0.32	0.001	0.46
84	0.001	0.001	0.288	0.078	0.01	0.264	0.001	0.42
85	0.001	0.001	0.196	0.058	0.012	0.256	0.001	0.45
86	0.001	0.002	0.184	0.174	0.002	0.476	0.001	0.43
87	0.001	0.008	0.3	0.06	0.002	0.722	0.001	0.51
88	0.001	0.01	0.106	0.128	0.008	0.548	0.001	0.53
89	0.001	0.001	0.312	0.048	0.001	0.044	0.001	0.47

90	0.001	0.002	0.248	0.052	0.012	0.33	0.001	0.47
91	0.001	0.001	0.302	0.144	0.042	0.808	0.001	0.45
92	0.001	0.002	0.284	0.084	0.01	0.366	0.001	0.42
93	0.001	0.001	0.334	0.136	0.014	0.27	0.001	0.43
94	0.002	0.001	0.094	0.03	0.016	0.068	0.001	0.50
95	0.001	0.001	0.122	0.048	0.022	0.294	0.001	0.45
96	0.001	0.001	0.4	0.058	0.002	0.158	0.001	0.42
97	0.012	0.001	0.17	0.06	0.002	0.506	0.001	0.57
98	0.001	0.001	0.452	0.022	0.016	0.172	0.001	0.44
99	0.001	0.001	0.186	0.042	0.028	0.562	0.001	0.47
100	0.001	0.001	0.248	0.034	0.002	0.006	0.001	0.50

Table S6.

Bayesian phylogenetic regression models predicting $D_{PATHWISE}$ and $NC_{PATHWISE}$ for Primates plus Plesiadapiformes. The best-fit regression, given the marginal likelihood and deviance information criterion, for each response variable, is at the bottom. GT = Global temperature, LT = Local temperature, LT_{RATE} = Pathwise rate local temperature, LP = Local precipitation, LP_{RATE} = Pathwise rate local precipitation, DIC = Deviance information criterion, MLh = Marginal likelihood estimated by stepping-stones. Beta parameters in black are significant, i.e., $P_{MCMC} < 0.05$. Beta parameters in grey are not significant, i.e., $P_{MCMC} > 0.05$.

Response	**Predictors**	**DIC**	**MLh**	**R^2**
$D_{PATHWISE}$	$\beta_0 + \beta_1(Time) + \beta_2(GT)$	-	761.84	0.06
	$\beta_0 + \beta_1(Time) + \beta_2(GT) + \beta_3(LT) + \beta_4(LP)$	-	767.09	0.11
	$\beta_0 + \beta_1(Time) + \beta_2(GT) + \beta_3(LT) + \beta_4(LT_{RATE}) + \beta_5(LP_{RATE})$	-	1199.41	0.68
$NC_{PATHWISE}$	$\beta_0 + \beta_1(Time) + \beta_2(GT)$	4920.33	-	0.43
	$\beta_0 + \beta_1(Time) + \beta_2(GT) + \beta_3(LT) - \beta_4(LP)$	4922.05	-	0.44
	$\beta_0 + \beta_1(Time) + \beta_2(GT) + \beta_3 (LT_{RATE}) + \beta_4(LP_{RATE})$	4864.24	-	0.61
	$\beta_0 + \beta_1(Time) + \beta_2(GT) + \beta_3(LP_{RATE})$	4862.87	-	0.61
	$\beta_0 + \beta_1(Time) + \beta_2(GT) - \beta_3(LT) + \beta_4(LP) + \beta_5(LP_{RATE})$	4856.98	-	0.62

Table S7.

Edited tip-names in the Euarchonta median tree.

MCC tree name	MCC tree dited name	Justification
Alouatta_coibensis	*Alouatta_palliata_coibensis*	Subspecies in the IUCN Red List
Alouatta_palliatus	*Alouatta_palliata_palliata*	Subspecies in the IUCN Red List
Avahi_betsilio	*Avahi_betsileo*	Typo
Avahi_ramanantsoavani	*Avahi_ramanantsoavanai*	Typo
Cercopithecus_albogularis	*Cercopithecus_mitis_albogularis*	Subspecies in the IUCN Red List
Cercopithecus_doggetti	*Cercopithecus_mitis_doggetti*	Subspecies in the IUCN Red List
Cercopithecus_dryas	*Chlorocebus_dryas*	Synonym in the IUCN Red List
Cercopithecus_kandti	*Cercopithecus_mitis_kandti*	Subspecies in the IUCN Red List
Chiropotes_israelita	*Chiropotes_sagulatus*	Synonym in the IUCN Red List
Lagothrix_cana	*Lagothrix_lagothricha_cana*	Subspecies in the IUCN Red List
Lagothrix_lagotricha	*Lagothrix_lagothricha_lagothricha*	Subspecies in the IUCN Red List
Lagothrix_lugens	*Lagothrix_lagothricha_lugens*	Subspecies in the IUCN Red List
Lagothrix_poeppigii	*Lagothrix_lagothricha_poeppigii*	Subspecies in the IUCN Red List
Lepilemur_sahamalazensis	*Lepilemur_sahamalaza*	Synonym in the IUCN Red List
Lepilemur_wrighti	*Lepilemur_wrightae*	Synonym in the IUCN Red List
Mico_humeralifera	*Mico_humeralifer*	Synonym in the IUCN Red List
Mico_humilis	*Callibella_humilis*	Synonym in the IUCN Red List
Otolemur_monteiri	*Otolemur_crassicaudatus_argentatus*	Monteiri and argentatus are synonyms and sub species of crassicaudatus but only argentatus has IUCN data.
Saguinus_graellsi	*Leontocebus_nigricollis_graellsi*	Synonym and subspecies in the IUCN Red List.
Theropithecus_sp_M2974_et_MP44	*Theropithecus_darti*	Synonym PBDB.
AnchomomysFendantia_pygmaeus	*Anchomomys_(Fendantia)_pygmaeus*	PBDB format-compatibility
AnchomomysHuerzeleris_quercyi	*Anchomomys_(Huerzeleris)_quercyi*	PBDB format-compatibility
HispanopithecusHispanopithecus_hungaricus	*Hispanopithecus_(Hispanopithecus)_hungaricus*	PBDB format-compatibility
HispanopithecusHispanopithecus_laietanus	*Hispanopithecus_(Hispanopithecus)_laietanus*	PBDB format-compatibility
LeptadapisParadapis_priscus	*Leptadapis_(Paradapis)_priscus*	PBDB format-compatibility
TheropithecusOmopithecus_brumpti	*Theropithecus_(Omopithecus)_brumpti*	PBDB format-compatibility

Table S8.

Number of random coordinates generated within the primate's distribution polygons.

Polygons area (Km^2)	Random coordinates (n)
≥ 20 < 100,000	50
≥ 100,000 < 200,000	100
≥ 200,000 < 300,000	200
≥ 300,000 < 400,000	300
≥ 400,000 < 500,000	400
≥ 500,000	500